EFFECTS OF STIFFENERS ON VIBRATIONS OF FIBER-REINFORCED AND LAMINATED COMPOSITE SHELLS

A Thesis Submitted to
the Graduate School of Engineering and Sciences of
İzmir Institute of Technology
in Partial Fulfillment of the Requirements for the Degree of

MASTER OF SCIENCE

in Mechanical Engineering

by
Tansel SARI

March 2018
İZMİR

We approve the thesis of **Tansel SARI**

Examining Committee Members:

Prof. Dr. Bülent YARDIMOĞLU
Department of Mechanical Engineering, İzmir Institute of Technology

Assoc. Prof. Dr. H. Seçil ARTEM
Department of Mechanical Engineering, İzmir Institute of Technology

Prof. Dr. Hasan ÖZTÜRK
Department of Mechanical Engineering, Dokuz Eylül University

09 March 2018

Prof. Dr. Bülent YARDIMOĞLU
Supervisor, Department of Mechanical Engineering,
İzmir Institute of Technology

Prof. Dr. Metin TANOĞLU
Head of the Department of
Mechanical Engineering

Prof. Dr. Aysun SOFUOĞLU
Dean of the Graduate School
of Engineering and Sciences

ACKNOWLEDGEMENTS

I would first like to thank my thesis advisor Professor Dr. Bülent YARDIMOGLU of the Department of Mechanical Engineering at Izmir Institute of Technology, for his support throughout my years of study and through the process of researching and writing this thesis. The door to Prof. Dr. YARDIMOGLU office was always open whenever I ran into a trouble spot or had a question about my research or writing. He consistently allowed this paper to be my own work, but steered me in the right the direction whenever he thought I needed it.

I must also express my very profound gratitude to my parents for providing me with unfailing support and continuous encouragement along my time in graduate school. This accomplishment would not have been possible without them.

ABSTRACT

EFFECTS OF STIFFENERS ON VIBRATIONS OF FIBER-REINFORCED AND LAMINATED COMPOSITE SHELLS

Vibration characteristics of fiber-reinforced and laminated composite paraboloidal shells with stiffeners are studied by Finite Element Method. The effects of stiffeners on natural frequencies are investigated by using a developed code in ANSYS. The developed code is verified by using several case studies on special cases of the present problem due to the lack of the present case in the reachable literature. Case studies are related with determination of natural frequencies of composite square plate, composite cylindrical shell, stiffened isotropic square plate, and isotropic paraboloidal shell of revolution. After validation of the developed computer code, effects of number of stiffener and cross-section of the stiffener on natural frequencies of fiber-reinforced and laminated composite paraboloidal shells are presented.

ÖZET

FEDERLERİN FİBER TAKVİYELİ VE TABAKALI KOMPOZİT KABUKLARIN TİTREŞİMLERİNE ETKİLERİ

Federlerleri olan fiber takviyeli ve tabakali kompozit paraboloid kabukların titreşim özellikleri Sonlu Elemanlar Yöntemi ile incelenmiştir. Federlerin doğal frekanslar üzerindeki etkileri ANSYS'de geliştirilmiş bir kod kullanılarak araştırılmıştır. Mevcut problemin ulaşılabilir literatürde olmaması nedeniyle, geliştirilen kod mevcut problemin özel durumları üzerine yapılmış birkaç durum çalışması kullanılarak doğrulanmıştır. Durum çalışmaları kompozit kare plaka, kompozit silindirik kabuk, federli izotropik kare plak ve izotropik parabolik kabuklarının doğal frekanslarının belirlenmesi ile ilgilidir. Geliştirilen bilgisayar kodunun doğrulanmasından sonra, feder sayısının ve federlerin enine kesitinin fiber takviyeli ve tabakalı kompozit parabolik kabukların doğal frekansları üzerindeki etkileri sunulmuştur.

TABLE OF CONTENTS

LIST OF FIGURES

Figure **Page**

LIST OF TABLES

Table **Page**

LIST OF SYMBOLS

A_{ij}	extensional stiffness
dA_2, dA_1	area elements perpendicular to ξ_1 and ξ_2 axes
B_{ij}	bending-extensional stiffness
D_{ij}	bending stiffnesses
E_1, E_2	Young's moduli in 1 and 2 material principal directions
G_{ij}	shear moduli in *i-j* surfaces, respectively
h	thickness of shell
I_i	i-th inertia
k	layer number
L_i	Lame' coefficients (i = 1, 2, 3)
M_i	moment resultants (i = 1, 2, 6)
m	number of terms
N	total number of layers in laminate
N_i	normal stress resultants (i = 1, 2, 6)
n	number of terms
P_i	rotary inertia
Q_i	shear stress resultants (i = 1, 2)
q_{mn}	coefficients in expansion of transverse load
R	position vector of point in shell
R_i	principal radii of curvature
r	position vector of point on shell midsurface
u_i	displacements of midsurface (i = 1, 2, 3)
$\overline{u}_i$	displacements of point in shell (i = 1, 2, 3)
α_i	surface metrics (z = 1, 2)
δ	variational operator
Φ_i	rotations about normal to shell midsurface
ε_i	strain components (i = 1, 2, 4, 5, 6)
θ	angle of material orientation
κ	curvature
ρ	density of the material

σ_i	stress components (i = 1, 2, 4, 5, 6)
ν_{ij}	Poisson's ratios
ξ_i	curvilinear coordinates in surface of shell
ζ	coordinate transverse to shell midsurface

CHAPTER 1

GENERAL INTRODUCTION

1.1. Literature Review

It is known that stiffened plates and shells exhibit superior performance in practical usage in different applications such as aircraft, ship, roof, submarine, bridge etc. In other words, usage of stiffeners in plates and shells provide the desired strength to mass ratio. Without classifying the shell and stiffener type, literature review on the aforementioned topic are presented in next paragraphs.

Hoppmann et al (1963, 1964) presented a discussion of the theory of vibration of a paraboloidal shell of revolution shown in Figure 1.1 that is associated with the work of Love (1944). They studied on the equations of motion considering both flexural and membrane stresses. Also, they performed the extensive experimental study of the vibrations of two models of thin paraboloidal shells.

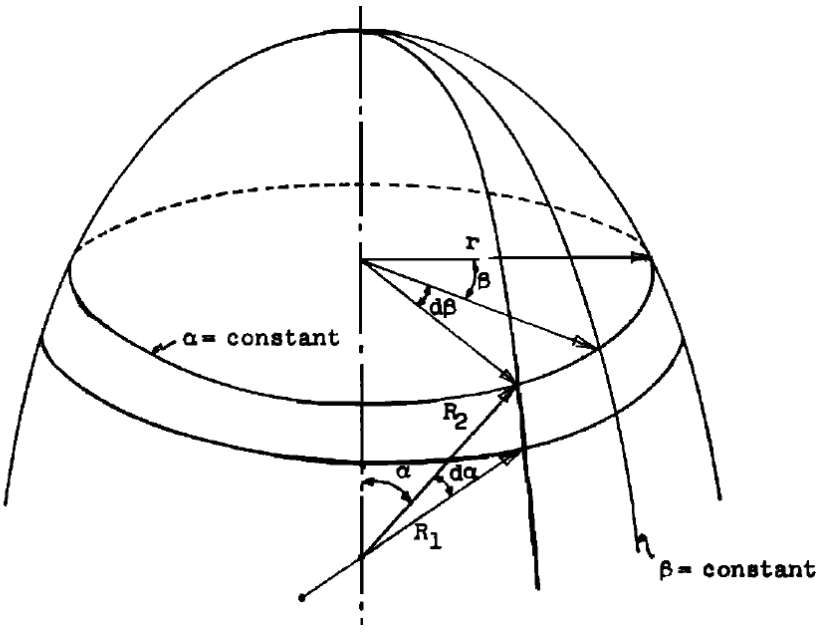

Figure 1.1. Paraboloidal shell of revolution
(Source: Hoppmann et al, 1964)

Mikulas and McElman (1965) derived dynamic equilibrium equations and boundary conditions from energy principles for eccentrically stiffened cylinder shown in Figure 1.2 and flat plates by neglegting the in-plane inertias. They obtained the frequency expressions for simple-support boundary conditions for both the cylinder and the plate. Then, they found that eccentricities may have a significant effect on natural frequencies.

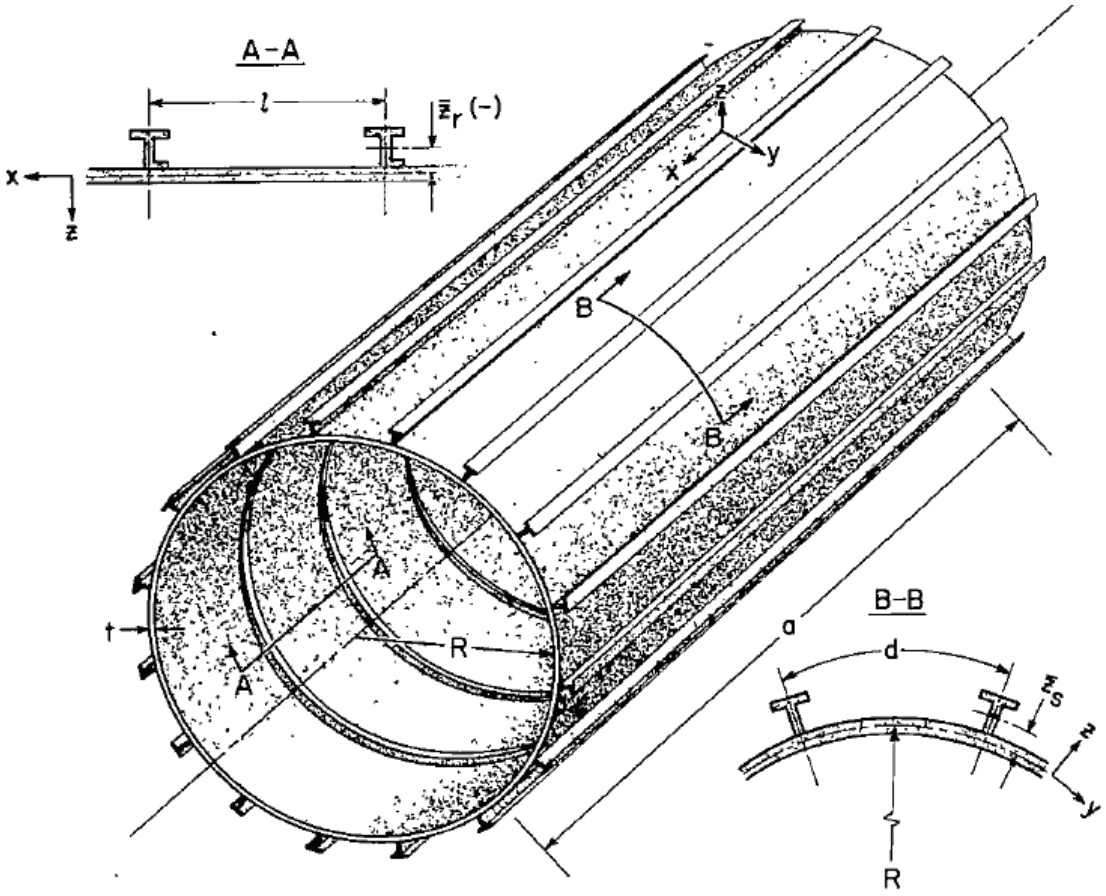

Figure 1.2. Geometry of eccentrically stiffened cylinder
(Source: Mikulas and McElman, 1965)

Bacon and Bert (1967) analyzed numerically free vibrations of shells of revolution for both axisymmetric and imsymmetric cases. They extended Love's first-approximation shell theory by including transverse-shear deformation and sandwich effects, and also translational and rotatory inertia. Their solution is based on Rayleigh-Ritz technique with three terms for each modal function for truncated-conical-shell elements as doubly curved shells of revolution. They studied for the axisymmetric and unsymmetric modes of a sandwich truncated conical shell and truncated paraboloid shell, respectively.

Sewall and Naumann (1968) presented the analytical and experimental results of vibration of cylindrical shells with and without external or internal integral longitudinal stiffeners as shown in Figure 1.3. Their analytical study is based on the Rayleigh-Ritz procedure. They concluded that the minimum frequencies of the externally stiffened shells are significantly higher than the minimum frequencies of the corresponding internally stiffened shells. Also, they found that the effect of stiffener rotatory inertia in the analysis is negligible. Although this study is mainly concerned with stringer-stiffened shells; two ring-stiffened shells are also considered to validate the averaged-stiffener assumption for the discussed configurations.

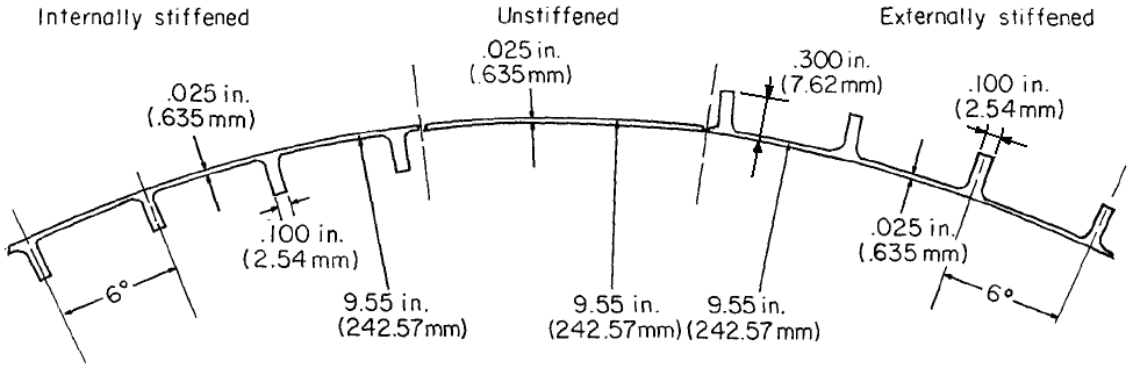

Figure 1.3. Geometrical and structural details of models
(Source: Sewall and Naumann, 1968)

Egle and Sewall (1968) developed a free vibration analysis for a ring-and-stringer-stiffened circular cylindrical shell, as shown in Figure 1.4, having various boundary conditions. They treated the stiffeners as discrete elements. They showed that stringers couple circumferential modes of different wave numbers and also couple symmetric and antisymmetric circumferential modes.

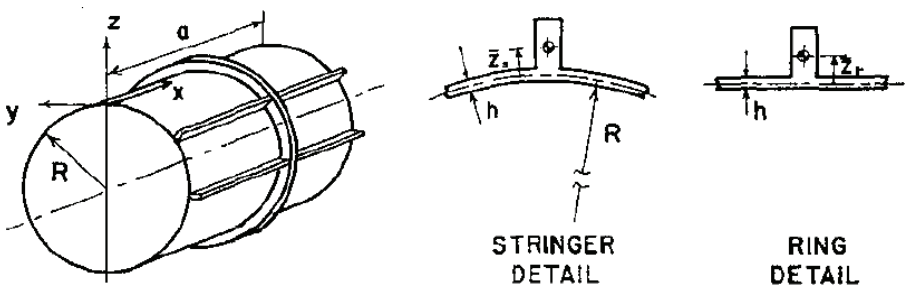

Figure 1.4. Model of discretely stiffened cylindrical shell
(Source: Egle and Sewall, 1968)

Naumann et al (1971) investigated the vibratory behavior of internally ring-stiffened truncated-cone shells by experimental and analytical methods. Figure 1.5 shows the rings before attached to the inner wall of the shell. In analytical method, linear thin-shell theory and the Rayleigh-Ritz method are employed.

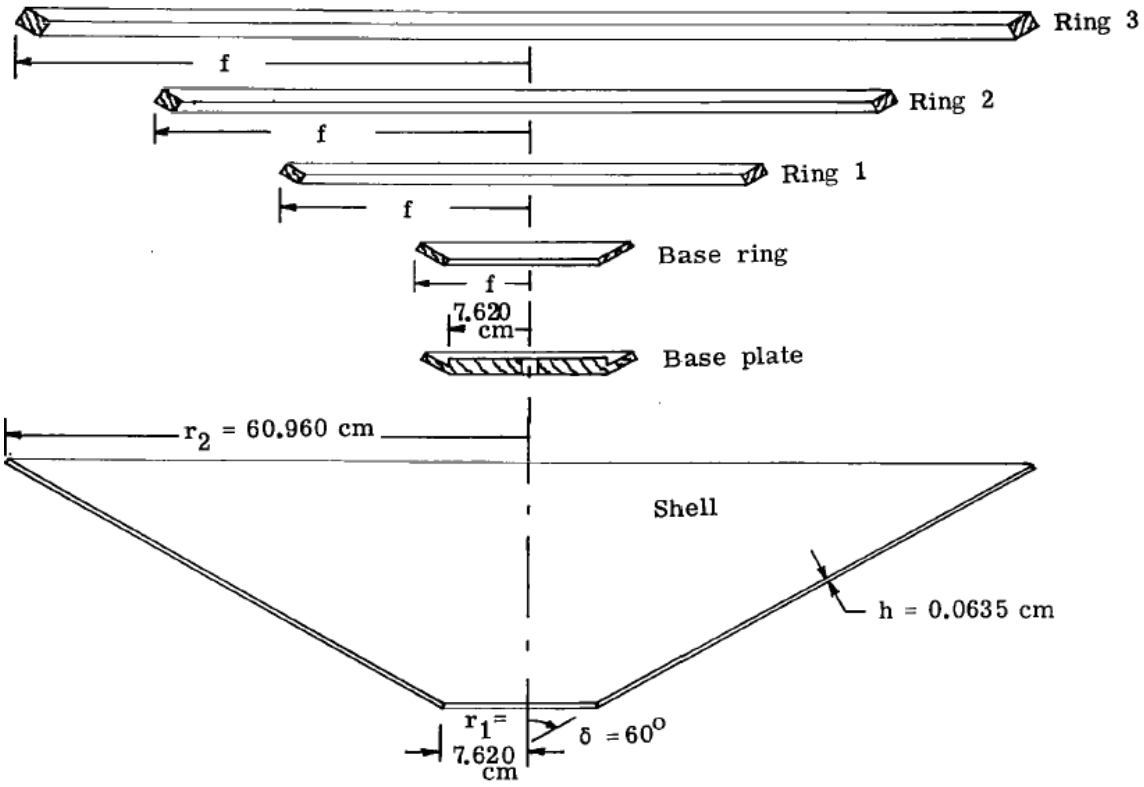

Figure 1.5. Schematic representations of model
(Source: Naumann et al, 1971)

Prokopenko (1979) presented the intrinsic oscillation frequency of a laminar reinforced cylindrical shell based on an energetics method. He studied on the effect of the number of reinforcing ribs and their thickness on the intrinsic oscillation frequency.

Venkatesh and Rao (1983) described a finite element analysis of laminated cylindrical shells with laminated stiffeners for stiffeners described in their paper. Later, Venkatesh and Rao (1985) extended their aforesaid study for laminated shells of revolution reinforced with laminated stiffeners.

Mustafa and Ali (1989) presented a method for the determination of natural frequencies of stiffened circular cylindrical shells considering the bending in two planes and rotary inertia of the stiffeners. Ring stiffened, stringer stiffened and orthogonally stiffened shells have been examined by using energy method.

Srinivasan and Krishnan (1989) interested in the analysis of dynamic response of stiffened conical shell panels by using an integral equation method. He studied on the effect of eccentricity of stiffeners by using the smearing technique for closely spaced stiffeners. The mode superposition method is used for the dynamic response analysis.

Bhimaraddi et al (1989) presented a finite element analysis of orthogonally stiffened laminated shells of revolution by combining isoparametric shell of revolution element and a isoparametric laminated curved beam element which take into account the effects of shear deformation and rotary.

Liao and Reddy (1990) developed a degenerate shell element with a degenerate curved beam element as a stiffener for the geometric nonlinear analysis of laminated, anisotropic, stiffened shells.

Bert and Kim (1993) analyzed free vibration characteristics of thin-walled circular cylindrical shells having composite materials and stiffeners in the form of ring and/or stringer. They presented numerical results for graphite-epoxy shells with stiffeners.

Goswami and Mukhopadhyay (1994) analysed composite stiffened shells by using two different elements which are incorporating shear deformation. Concentric and eccentric stiffened composite shells have been analyzed.

Raj et al (1995) reported the effects of stiffeners on vibration of conical shell models with and without circumferential ring stiffeners by both theoretical and experimental methods.

Sinha and Mukhopadhyay (1995) presented a review on the static and dynamic analysis of stiffened shells.

Huang and Chen (1996) employed a modified receptance method for the vibration analysis of a spinning cylindrical shell with internal, symmetric, or external ring stiffeners. They discussed the effects of types, numbers of stiffeners and of spin speed on the shell frequencies.

Lee and Kim (1998) used the energy method for the analytical solutions of the free vibration analysis of the rotating composite cylindrical shells with axial and circumferential stiffeners. They employed the Love's shell theory based on the discrete stiffener theory. They studied on the effect of the geometric parameters of the stiffeners on natural frequencies.

Gunay (1999) developed a finite element model for an anisotropic thin/thick shallow laminated shell with stringer-type stiffeners.

Prusty and Satsangi (2001) presented a modified approach of a curved shear flexible element. They carried out a static analysis for stiffened shells by using an eight-noded isoparametric finite element for the shell and a three-noded curved beam element for the stiffener.

Ruotolo (2001) compared the Donnell's, Love's, Sanders' and Flügge's thin shell theories in the evaluation of natural frequencies of cylinders stiffened with rings and stringers. He used the smeared approach for stiffeners. He concluded that Donnell's theory gives highly inaccurate results with respect to the other three theories.

Zhao et al (2002) used energy method for vibration analysis of simply supported rotating cross-ply laminated cylindrical shells with stringers and rings. They considered the effects of initial hoop tension, centrifugal and Coriolis forces due to the rotation. Moreover, eccentricity of stiffener is taken into account.

Prusty (2003) presented a linear static analysis of laminated composite panels with the hat-shaped stiffener shown in Figure 1.6 by using finite elements.

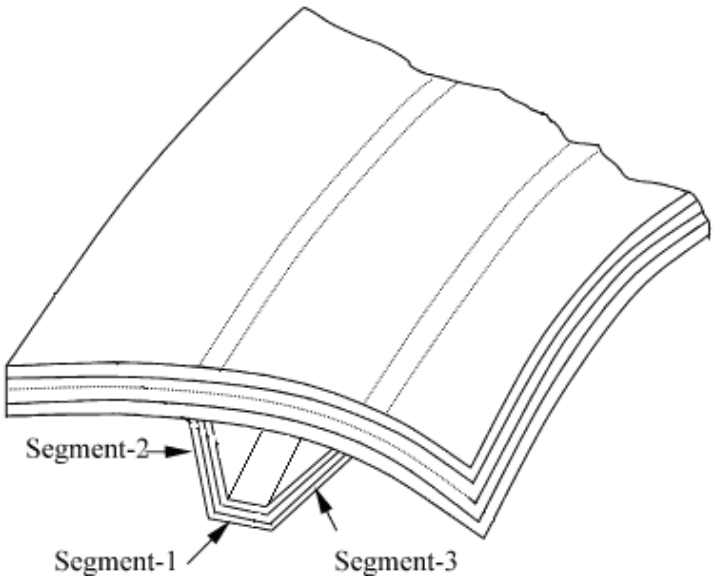

Figure 1.6. Laminated hat stiffened shell showing stiffener segments
(Source: Prusty, 2003)

Jafari and Bagheri (2006) investigated the free vibration analysis of simply supported cylindrical shells with circumferential stiffeners with non-uniform stiffeners eccentricity and unequal stiffeners spacing by using analytical method based on Ritz method, experimental modal analysis, and finite elements models employing shell and beam elements in ANSYS.

Pan et al (2008) studied on the vibration of ring-stiffened cylinders with arbitrary boundary conditions. They adopted the classical linear shell theory of Flugge (1934) along with the trigonometric functions for displacements of cylinders and used ‘‘smeared frame’’ approach for ring-type stiffeners.

Torkamani et al (2009) developed scaling laws for free vibrations of orthogonally stiffened cylindrical shells, shown in Figure 1.7, using the similitude theory that is applied to for vibrating thin shells by Soedel (1971). They used the Donnell-type nonlinear strain-displacement relations along with the smearing theory.

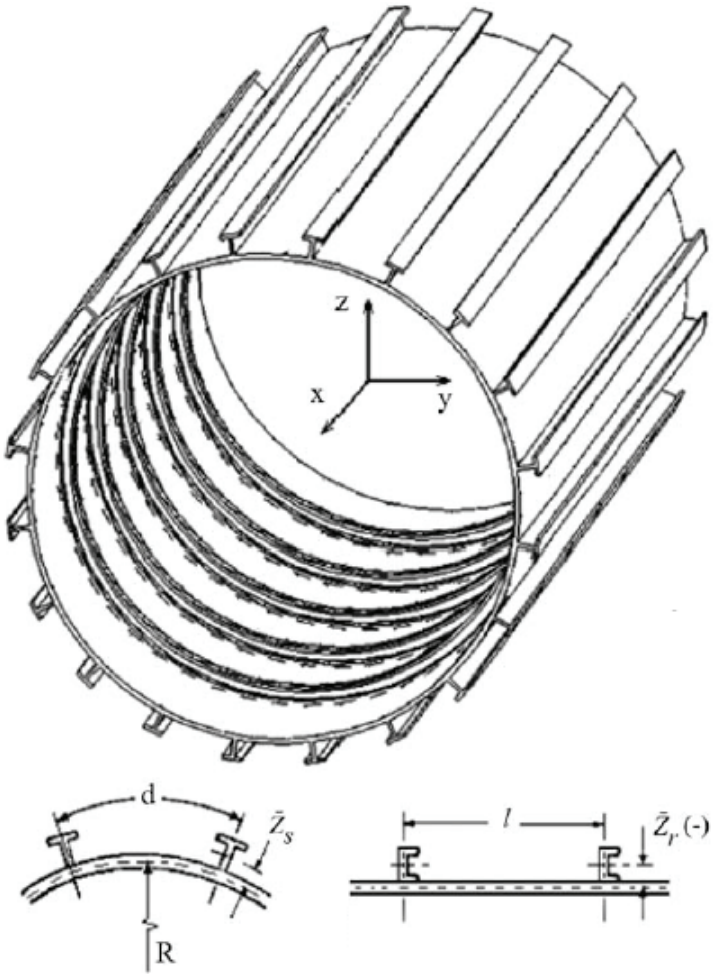

Figure 1.7. Geometry of a typical orthogonally stiffened cylindrical shell
(Source: Torkamani et al, 2009)

Gan et al (2009) used the wave propagation approach to analyze the free vibration of ring-stiffened cylindrical shell based on Flugge (1973) classical thin shell theory and the smeared approach.

Luan et al (2011) combined the improved smeared plate technique with the equation of motion for a doubly curved thin rectangular shell. They validated their prediction technique by comparing natural frequencies, mode shapes, and forced responses from simulation results with the results from experiments of a doubly curved cross-stiffened shell.

Edalat et al (2013) focused on the dynamic response and free vibration analysis of stiffened shells with parabolic curvatures, shown in Figure 1.8, by using the equivalent structure approach. They employed energy method to determine of the equivalent orthotropic shell parameters of parabolic stiffened shells. Their longitudinal stiffener arrangements in shell are shown in Figure 1.9.

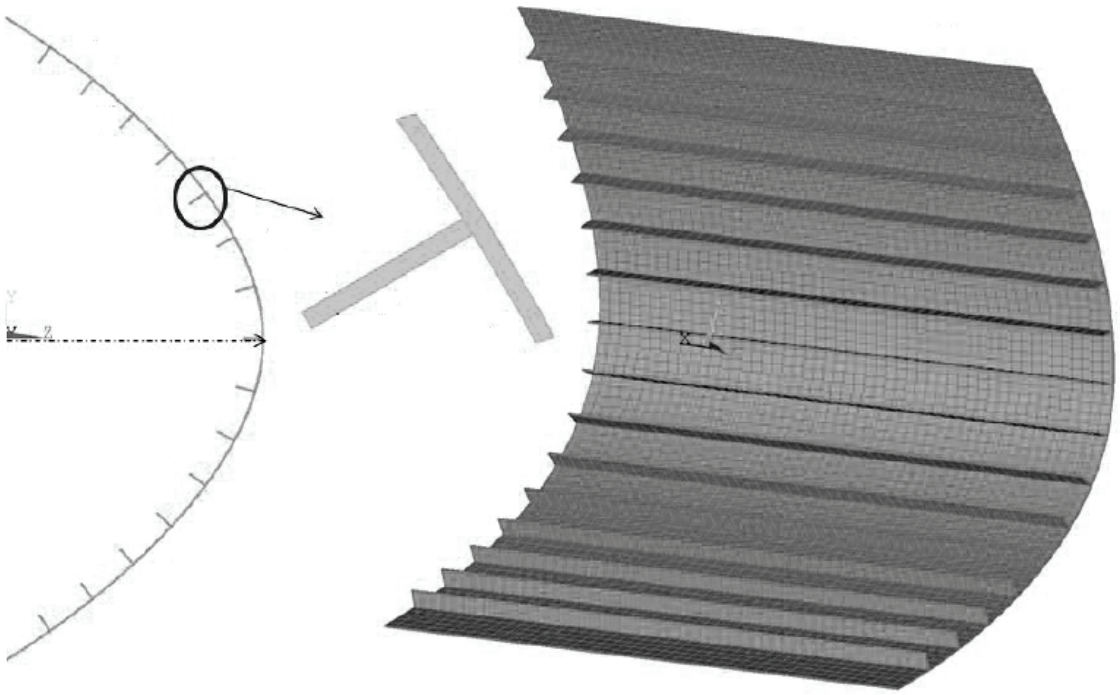

Figure 1.8. Finite element model of stiffened shells with parabolic curvatures
(Source: Edalat et al, 2013)

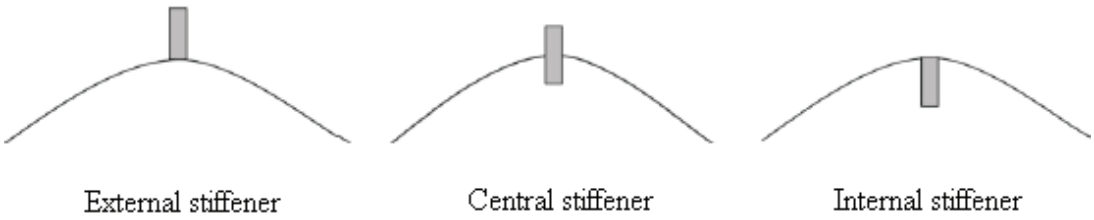

Figure 1.9. Longitudinal stiffener arrangement in shell
(Source: Edalat et al, 2013)

1.2. Objectives of the Study

Objective of this study is to determine the effects of stiffeners on vibration analysis of fiber-reinforced and laminated composite paraboloidal shells. A critical damage of this type of structure has been experienced due to the heavy rainfall in the plane flying at 4,000 ft as shown in Figure 1.10.

Due to the complexity of the geometrical properties and mathematical model of the stiffened shell structure, finite element method is employed to study the current topic. A commonly used finite element package ANSYS is used to model and solve the problem. A computer code is developed by using APDL (ANSYS Parametric Design Language) in ANSYS. The developed code is confirmed by using several case studies available in the reachable literature. After validation of the developed computer code, effects of number of stiffener and cross-section of the stiffener on natural frequencies of fiber-reinforced and laminated composite paraboloidal shells are presented.

Figure 1.10. Airplane damaged by nose and windshield during hailstorm
(Source: QHA, 2017)

CHAPTER 2

THEORETICAL BACKGROUND

2.1. Theory of Shell

In this thesis, the first-order shear deformation theory of shell is presented. The differential element of a doubly curved shell with orthogonal curvilinear coordinate is shown in Figure 2.1. R_1 and R_2 are the principal radii of the middle surface. Also, dA_1 and dA_2 are elements of area of cross sections.

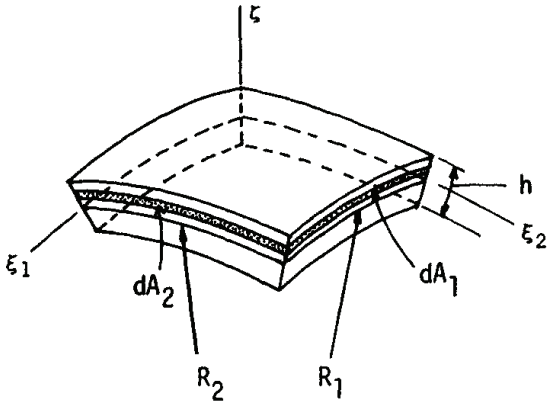

Figure 2.1. Differential element of a doubly curved shell
(Source: Reddy, 1984)

The position vectors $\vec{r}$ and $\vec{R}$ are used to represent any point on the middle surface and any point at the distance ζ from the middle surface, respectively.

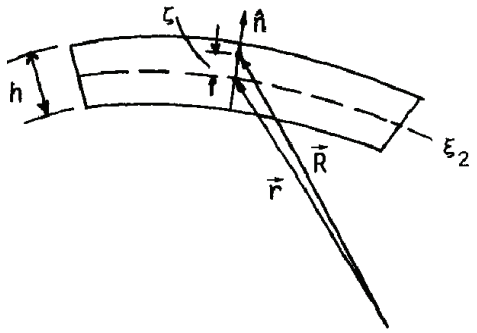

Figure 2.2. Position vectors $\vec{r}$ and $\vec{R}$
(Source: Reddy, 1984)

The differential distance vector of two points on the middle surface is written as

$$d\vec{r} = \vec{r}_1 d\xi_1 + \vec{r}_2 d\xi_2 \tag{2.1}$$

where

$$\vec{r}_1 = \partial\vec{r} / \partial\xi_1 \ , \qquad \vec{r}_2 = \partial\vec{r} / \partial\xi_2 \tag{2.2}$$

Thus, the differential distance *ds* between two points on the middle surface is expressed as

$$(ds)^2 = d\vec{r}.d\vec{r} = \alpha_1^2 (d\xi_1)^2 + \alpha_2^2 (d\xi_2)^2 \tag{2.3}$$

where α_1 and α_2 are surface metrics and defined by

$$\alpha_1^2 = \vec{r}_1.\vec{r}_1 \quad , \qquad \alpha_2^2 = \vec{r}_2.\vec{r}_2 \tag{2.4}$$

Similarly, the differential distance vector of two points on the surface at the distance ζ from the middle surface is written as

$$d\vec{R} = (\partial\vec{R} / \partial\xi_1) d\xi_1 + (\partial\vec{R} / \partial\xi_2) d\xi_2 + (\partial\vec{R} / \partial\varsigma) d\varsigma \tag{2.5}$$

and the differential distance *dS* is obtained as

$$(dS)^2 = d\vec{R}.d\vec{R} = L_1^2 (d\xi_1)^2 + L_2^2 (d\xi_2)^2 + L_3^2 (d\varsigma)^2 \tag{2.6}$$

where L_1, L_2 and L_3 are Lame' coefficients and defined by

$$L_1 = \alpha_1 (1 + \varsigma / R_1) \tag{2.7}$$

$$L_2 = \alpha_2 (1 + \varsigma / R_2) \tag{2.8}$$

$$L_3 = 1 \tag{2.9}$$

Therefore, the elements of area of cross sections dA_1 and dA_2 are given by

$$dA_1 = L_1 d\xi_1 d\varsigma = \alpha_1 (1 + \varsigma / R_1) d\xi_1 d\varsigma \tag{2.10}$$

$$dA_2 = L_2 d\xi_2 d\varsigma = \alpha_2 (1 + \varsigma / R_2) d\xi_2 d\varsigma \tag{2.11}$$

The stress resultants of a shell element are illustrated in Figure 2.3.

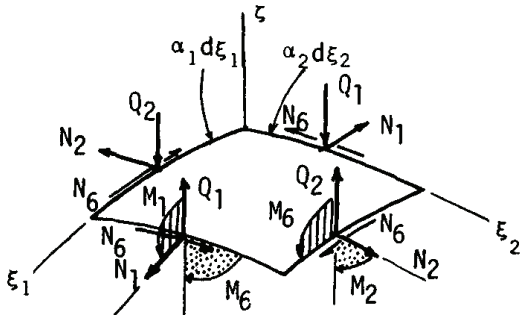

Figure 2.3. Stress resultants of a shell element
(Source: Reddy, 1984)

They are given by Reddy (1984) as follows:

$$\begin{Bmatrix} N_1 \\ N_2 \\ N_{12} \\ N_{21} \\ Q_1 \\ Q_2 \\ M_1 \\ M_2 \\ M_{12} \\ M_{21} \end{Bmatrix} = \int_{-h/2}^{h/2} \begin{Bmatrix} \sigma_1 (1 + \varsigma / R_2) \\ \sigma_2 (1 + \varsigma / R_1) \\ \sigma_6 (1 + \varsigma / R_2) \\ \sigma_6 (1 + \varsigma / R_1) \\ \sigma_5 (1 + \varsigma / R_2) \\ \sigma_4 (1 + \varsigma / R_1) \\ \varsigma\sigma_1 (1 + \varsigma / R_2) \\ \varsigma\sigma_2 (1 + \varsigma / R_1) \\ \varsigma\sigma_6 (1 + \varsigma / R_2) \\ \varsigma\sigma_6 (1 + \varsigma / R_1) \end{Bmatrix} d\varsigma \tag{2.12}$$

Since ξ / R_1 and ξ / R_2 are negligable in comparison with unity for thin shells (h/R_1, h/R_2 less than 1/20), N_{12} and N_{21} are equal to N_6 and M_{12} and M_{21} are equal to M_6.

The displacement fields based on the first-order shear deformation theory are given by Reddy (1984) as

$$\bar{u}_1 = \frac{1}{\alpha_1}(L_1 u_1) + \varsigma\phi_1 \tag{2.13}$$

$$\bar{u}_2 = \frac{1}{\alpha_2}(L_2 u_2) + \varsigma\phi_2 \tag{2.14}$$

$$\bar{u}_3 = u_3 \tag{2.15}$$

where $(\bar{u}_1, \bar{u}_2, \bar{u}_3)$ is the displacements of a point (ξ_1,ξ_2,ζ) along the (ξ_1,ξ_2,ζ) coordinates; and (u_1, u_2, u_3) is the displacements of a point $(\xi_1,\xi_2,0)$. The following strain-displacement relations are obtained by substituting Equations (2.13)-(2.15) into the strain-displacement relations of an orthogonal curvilinear coordinate system,

$$\varepsilon_i = \varepsilon_i^0 + \varsigma\kappa_i, \;\; i = 1,2,6 \tag{2.16}$$

$$\varepsilon_i = \varepsilon_i^0, \qquad i = 4,5 \tag{2.17}$$

where

$$\varepsilon_1^0 = \frac{1}{\alpha_1}\frac{\partial u_1}{\partial \xi_1} + \frac{u_3}{R_1} \tag{2.18}$$

$$\varepsilon_2^0 = \frac{1}{\alpha_2}\frac{\partial u_2}{\partial \xi_2} + \frac{u_3}{R_2} \tag{2.19}$$

$$\varepsilon_4^0 = \frac{1}{\alpha_2}\frac{\partial u_3}{\partial \xi_2} + \phi_2 - \frac{u_2}{R_2} \tag{2.20}$$

$$\varepsilon_5^0 = \frac{1}{\alpha_1}\frac{\partial u_3}{\partial \xi_1} + \phi_1 - \frac{u_1}{R_1} \tag{2.21}$$

$$\varepsilon_6^0 = \frac{1}{\alpha_1}\frac{\partial u_2}{\partial \xi_1} + \frac{1}{\alpha_2}\frac{\partial u_1}{\partial \xi_2} \tag{2.22}$$

$$\kappa_1 = \frac{1}{\alpha_1}\frac{\partial \phi_1}{\partial \xi_1} \tag{2.23}$$

$$\kappa_2 = \frac{1}{\alpha_2}\frac{\partial \phi_2}{\partial \xi_2} \tag{2.24}$$

$$\begin{aligned}\kappa_6 = {} & \frac{1}{\alpha_1}\frac{\partial \phi_2}{\partial \xi_1} + \frac{1}{\alpha_2}\frac{\partial \phi_1}{\partial \xi_2} \\ & + \frac{1}{2}\left(\frac{1}{R_2} - \frac{1}{R_1}\right)\left(\frac{1}{\alpha_1}\frac{\partial u_2}{\partial \xi_1} - \frac{1}{\alpha_2}\frac{\partial u_1}{\partial \xi_2}\right)\end{aligned} \tag{2.25}$$

in which ϕ_1 and ϕ_2 are the rotations of the reference surface, $\varsigma = 0$, about the ξ_2- and ξ_1-coordinate axes, respectively.

2.2. Mechanics of Lamina

The shell and material coordinate systems of *k*th lamina is illustrated in Figure 2.4. As seen in figure, the principle material 1 axis is oriented at the angle θ from the shell 1 axis in the counterclockwise sense.

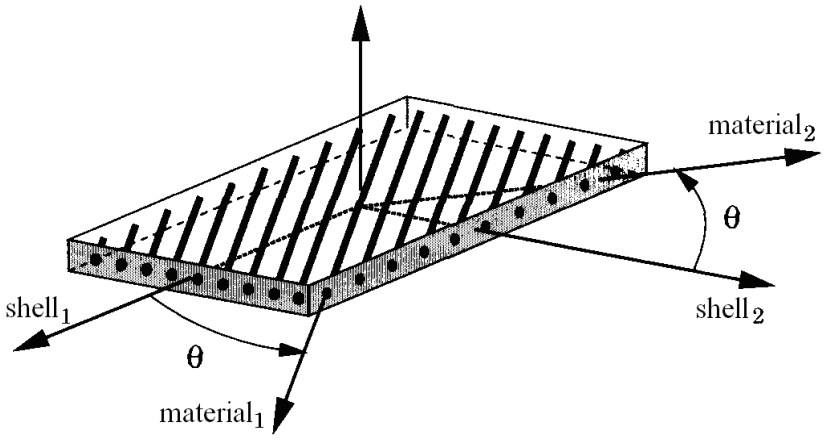

Figure 2.4. Coordinate systems for a typical lamina (modified)
(Source: Reddy, 2004)

The stress–strain relations of the *k*th lamina in the shell coordinate system in terms of the parameters known in material coordinate system is given in matrix form as (Reddy, 2004)

$$\begin{Bmatrix}\sigma_1\\ \sigma_2\\ \sigma_4\\ \sigma_5\\ \sigma_6\end{Bmatrix}^{(k)} = \begin{bmatrix}\overline{Q}_{11} & \overline{Q}_{12} & 0 & 0 & \overline{Q}_{16}\\ \overline{Q}_{12} & \overline{Q}_{22} & 0 & 0 & \overline{Q}_{26}\\ 0 & 0 & \overline{Q}_{44} & \overline{Q}_{45} & 0\\ 0 & 0 & \overline{Q}_{45} & \overline{Q}_{55} & 0\\ \overline{Q}_{16} & \overline{Q}_{26} & 0 & 0 & \overline{Q}_{66}\end{bmatrix}^{(k)} \begin{Bmatrix}\varepsilon_1\\ \varepsilon_2\\ \varepsilon_4\\ \varepsilon_5\\ \varepsilon_6\end{Bmatrix}^{(k)} \tag{2.26}$$

where $\overline{Q}_{ij}$ are the transformed stiffnesses of *k*th layer and given by using the notation *c*=Cos(θ), *s*=Sin(θ), and also omitting the supercript (*k*) for brevity as follows:

$$\overline{Q}_{11} = Q_{11}c^4 + Q_{22}s^4 + 2(Q_{12} + 2Q_{66})s^2c^2 \tag{2.27}$$

$$\overline{Q}_{12} = (Q_{11} + Q_{22} - 4Q_{66})s^2c^2 + Q_{12}(c^4 + s^2) \tag{2.28}$$

$$\overline{Q}_{22} = Q_{11}s^4 + Q_{22}c^4 + 2(Q_{12} + 2Q_{66})s^2c^2 \tag{2.29}$$

$$\overline{Q}_{16} = (Q_{11} - Q_{12} - 2Q_{66})sc^3 - (Q_{22} - Q_{12} - 2Q_{66})s^3c \tag{2.30}$$

$$\overline{Q}_{26} = (Q_{11} - Q_{12} - 2Q_{66})cs^3 - (Q_{22} - Q_{12} - 2Q_{66})sc^3 \tag{2.31}$$

$$\overline{Q}_{66} = (Q_{11} + Q_{22} - 2Q_{12} - 2Q_{66})c^2s^2 + Q_{66}(s^4 + c^4) \tag{2.32}$$

$$\overline{Q}_{44} = Q_{44}c^2 + Q_{55}s^2 \tag{2.33}$$

$$\overline{Q}_{45} = (Q_{55} - Q_{44})sc \tag{2.34}$$

$$\overline{Q}_{55} = Q_{55}c^2 + Q_{44}s^2 \tag{2.35}$$

in which Q_{ij} are the lamina stiffnesses referred to the principal material coordinates of the *k*th lamina and given by

$$Q_{11} = \frac{E_1}{1 - \upsilon_{21}\upsilon_{12}} \tag{2.36}$$

$$Q_{12} = \frac{\upsilon_{12}E_2}{1 - \upsilon_{21}\upsilon_{12}} \tag{2.37}$$

$$Q_{22} = \frac{E_2}{1 - \upsilon_{21}\upsilon_{12}} \tag{2.38}$$

$$Q_{44} = G_{23} \tag{2.39}$$

$$Q_{55} = G_{13} \tag{2.40}$$

$$Q_{66} = G_{12} \tag{2.41}$$

where E_1, E_2, G_{12}, G_{13}, G_{23}, v_{12}, and v_{21} are modulus of elasticities, shear modulus of elasticities and Poisson's ratios in the directions denoted by subscripts.

2.3. Mechanics of Laminated Composite Shells

If shell is composed of orthotropic layers as shown in Figure 2.5.a, the stress resultants of a shell element are expressed by using mechanics of composite materials.

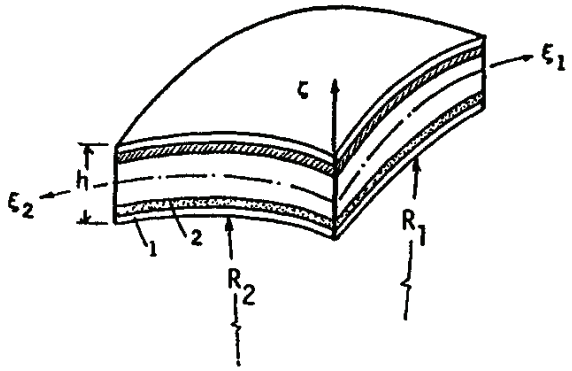

Figure 2.5. Geometry of laminated shell
(Source: Reddy, 1984)

Therefore, the stress resultants given in Equation (2.12) can be expressed as (Reddy, 2004)

$$\begin{Bmatrix} \{N\} \\ \{M\} \end{Bmatrix} = \begin{bmatrix} [A] & [B] \\ [B] & [D] \end{bmatrix} \begin{Bmatrix} \{\varepsilon^0\} \\ \{\kappa\} \end{Bmatrix} \tag{2.42}$$

$$\begin{Bmatrix} Q_2 \\ Q_1 \end{Bmatrix} = K_S \begin{bmatrix} A_{44} & A_{45} \\ A_{45} & A_{55} \end{bmatrix} \begin{Bmatrix} \varepsilon_4^0 \\ \varepsilon_5^0 \end{Bmatrix} \tag{2.43}$$

where the matrices [*A*], [*B*], and [*D*] are known as the extensional, coupling, and bending stiffness matrices, respectively. Their elements are expressed as

$$A_{ij} = \sum_{k=1}^{N} \overline{Q}_{ij}^{(k)} (\varsigma_{k+1} - \varsigma_k), \quad i, j = 1,2,6 \tag{2.44}$$

$$B_{ij} = \frac{1}{2} \sum_{k=1}^{N} \overline{Q}_{ij}^{(k)} (\varsigma_{k+1}^2 - \varsigma_k^2), \quad i, j = 1,2,6 \tag{2.45}$$

$$D_{ij} = \frac{1}{3} \sum_{k=1}^{N} \overline{Q}_{ij}^{(k)} (\varsigma_{k+1}^3 - \varsigma_k^3), \quad i, j = 1,2,6 \tag{2.46}$$

$$A_{ij} = \sum_{k=1}^{N} \overline{Q}_{ij}^{(k)} (\varsigma_{k+1} - \varsigma_k), \quad i, j = 4,5 \tag{2.47}$$

in which N is the number of layers in the shell, and ζ_{k+1} and ζ_k are the top and bottom ζ-coordinates of the kth lamina. Also, K_S is the shear correction factor.

The equations of motion are given by Reddy (2004) as

$$\frac{\partial N_1}{\partial x_1} + \frac{\partial}{\partial x_2}(N_6 + C_0 M_6) + \frac{Q_1}{R_1} = I_0 \frac{\partial^2 u_0}{\partial t^2} + I_1 \frac{\partial^2 \phi_1}{\partial t^2} \tag{2.48}$$

$$\frac{\partial}{\partial x_1}(N_6 - C_0 M_6) + \frac{\partial N_2}{\partial x_2} + \frac{Q_2}{R_2} = I_0 \frac{\partial^2 v_0}{\partial t^2} + I_1 \frac{\partial^2 \phi_2}{\partial t^2} \tag{2.49}$$

$$\frac{\partial Q_1}{\partial x_1}+\frac{\partial Q_2}{\partial x_2}-\left(\frac{N_1}{R_1}+\frac{N_2}{R_2}\right)+q=I_1\frac{\partial^2 w_0}{\partial t^2} \tag{2.50}$$

$$\frac{\partial M_1}{\partial x_1}+\frac{\partial M_6}{\partial x_2}-Q_1=I_2\frac{\partial^2 \phi_1}{\partial t^2}+I_1\frac{\partial^2 u_0}{\partial t^2} \tag{2.51}$$

$$\frac{\partial M_6}{\partial x_1}+\frac{\partial M_2}{\partial x_2}-Q_2=I_2\frac{\partial^2 \phi_2}{\partial t^2}+I_1\frac{\partial^2 v_0}{\partial t^2} \tag{2.51}$$

where

$$C_0=\frac{1}{2}\left(\frac{1}{R_1}-\frac{1}{R_2}\right) \tag{2.52}$$

$$\frac{1}{\partial x_i}\equiv\frac{1}{\alpha_i}\frac{1}{\partial \xi_i},\ i=1,2 \tag{2.53}$$

$$I_i=\sum_{k=1}^{N}\int_{\varsigma_k}^{\varsigma_{k+1}}\rho^{(k)}(\varsigma)^i\,d\varsigma,\ i=0,1,2 \tag{2.54}$$

2.4. Mechanics of Stiffeners

Curved beams are used as stiffeners in doubly curved shells. An example of orthogonally stiffened doubly curved shell is depicted in Figure 2.6.

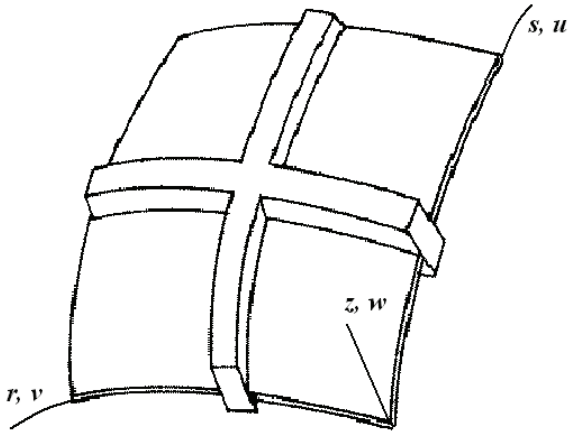

Figure 2.6. Doubly curved shell with orthogonal stiffeners

The stiffener arrangements in shell are introduced in Figure 1.9 as external, central, and internal stiffeners. According to this classification, Figure 2.6 shows central stiffeners. The displacements of middle surface of shell and central axis of curved beam are the same for the centrally located stiffeners. If the stiffeners have an eccentricity due to the locating of the central axis of the curved beam, it is considered in displacement field of curved beam axis.

The stiffener in the direction *s* shown in Figure 2.6 is considered. Coordinates of a curved beam is depicted in Figure 2.7. The axial, radial, and rotational displacements of curved beam are given in Figure 2.8 (Cook, 1989).

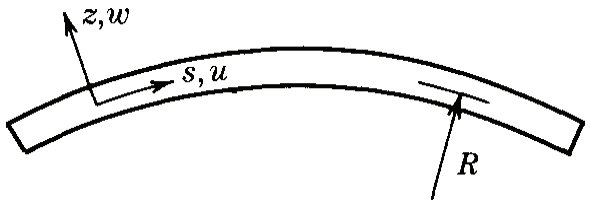

Figure 2.7. Coordinates of curved beam
(Source: Cook, 1989)

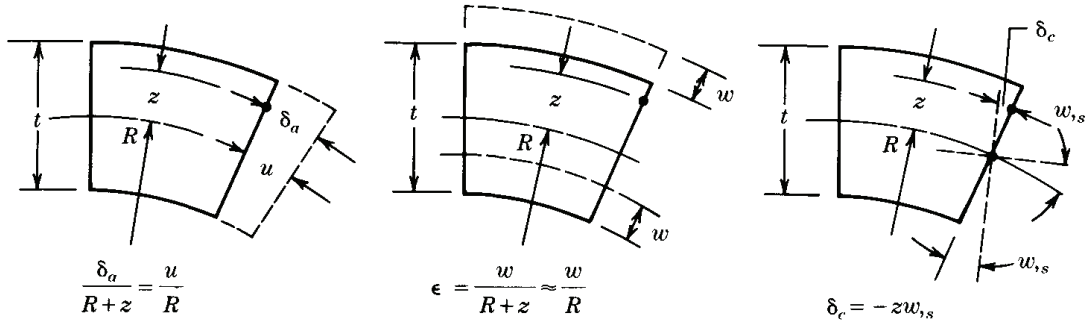

a. Axial displacement b. Radial displacement c. Rotational displacement

Figure 2.8. Displacements of a curved beam
(Source: Cook, 1989)

Using the formulations expressed in Figure 2.8, the strain of curved beam in circumferential direction is written as (Cook, 1989)

$$\begin{aligned}\varepsilon_s &= \frac{\partial}{ds}(\delta_a + \delta_c) + \frac{w}{R} \\ &= \frac{\partial u}{\partial s} + \frac{w}{R} + z\left(\frac{1}{R}\frac{\partial u}{\partial s} - \frac{\partial^2 w}{\partial s^2}\right)\end{aligned} \tag{2.55}$$

If the approximation $\delta_a \approx u$ is introduced, the first term inside of the parenthesis disappears. Equation (2.55) can be written alternatively as

$$\varepsilon_s = \varepsilon_m + z\kappa \tag{2.56}$$

where

$$\varepsilon_m = \frac{\partial u}{\partial s} + \frac{w}{R} \tag{2.57}$$

$$\kappa = \frac{1}{R}\frac{\partial u}{\partial s} - \frac{\partial^2 w}{\partial s^2} \tag{2.58}$$

in which ε_m and κ are membrane strain and change of curvature, respectively.

The stiffener in the direction *s* is affected from the deformation in direction *r* shown in Figure 2.6. In order to show this effect, geometrical interpretation of twisting of middle surface of shell is shown in Figure 2.9 (Yardimoglu, 2016).

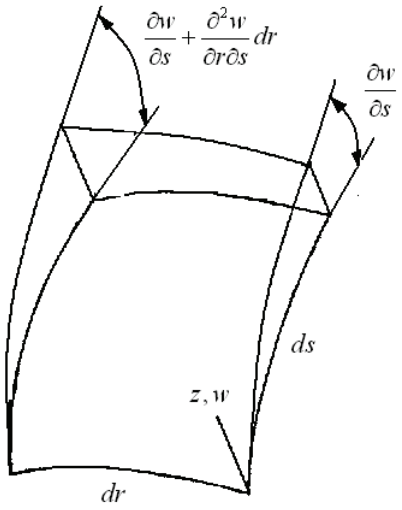

Figure 2.9. Geometrical interpretation of twisting of middle surface of shell

Therefore, the curved beam on hand has twisting as follows:

$$\tau = \frac{\partial^2 w}{\partial r \partial s} \tag{2.59}$$

2.5. Strain and Kinetic Energies of Stiffened Shells

In order to express the strain energy of laminated shell, Equation (2.26) may be written in closed form as

$$\{\sigma\}^{(k)} = \{\overline{Q}\}^{(k)}\{\varepsilon\}^{(k)} \tag{2.60}$$

Thus, the strain energy of laminated shell composed by *N* layer is written as

$$U_{shell} = \frac{1}{2}\sum_{k=1}^{N}\int_{V}\{\sigma\}^{T}\{\varepsilon\}dV \tag{2.61}$$

Kinetic energy of shell is written as

$$T_{shell} = \frac{1}{2}\sum_{k=1}^{N}\int_{V}\rho^{(k)}(\dot{\overline{u}}_1^2 + \dot{\overline{u}}_2^2 + \dot{\overline{u}}_3^2)dV \tag{2.62}$$

where $\dot{\overline{u}}_i$ is the velocity of the any point of the shell in direction *i*.

On the other hand, the strain and kinetic energies of a stiffener in the direction *s* can be expressed as (Egle and Sewall, 1968)

$$U_{ring} = \frac{1}{2}\sum_{k=1}^{m}\{\int_0^s E_m\int_{Area}\varepsilon_s^2 dA_m ds + (GJ)_m\int_0^s \tau^2 ds\} \tag{2.63}$$

$$\begin{aligned} T_{ring} = {} & \frac{1}{2}\sum_{k=1}^{m}\rho_m A_m\int_0^s[(\dot{u} - z_m\dot{w}_s)^2 + \\ & (\dot{v} - z_m\dot{w}_r)^2 + \dot{w}^2 + p_m^2\dot{w}_r^2 + d_m^2\dot{w}_s^2)ds \end{aligned} \tag{2.64}$$

where *m* is the number of ring in direction *s*. Other notations are listed in the Notation part of this thesis. The strain energies of other rings in direction *r* can be written similarly.

2.6. Modal Analysis by Finite Element Method

The equation of motion for multi-degree-of-freedom system for free vibration is written as

$$[M]\{\ddot{x}(t)\} + [K]\{x(t)\} = \{0\} \tag{2.65}$$

where $[M]$ and $[K]$ are mass and stiffness matrices, respectively. Also, $\{x(t)\}$ is displacement vector. In order to find the vibration characteristics of the discrete system, the generalized eigenvalue equation is obtained by substituting a harmonic response function $\{x(t)\} = \{X\}\sin\omega t$ in Equation (2.65). Thus, the generalized eigenvalue problem is obtained as

$$([K] - \omega_i^2[M])\{u_i\} = \{0\} \tag{2.66}$$

where ω_i is i^{th} natural frequency and $\{u_i\}$ is the i^{th} vibration mode shape vector.

Solution of Equation (2.66) is known as "Modal Analysis". Some of the mode-extraction methods available in ANSYS are given below:

- Block Lanczos (default): This method is used for large symmetric eigenvalue problems and uses the sparse matrix solver.
- Subspace: This method is also used for large symmetric eigenvalue problems. Several subspace iteration processes such as the frontal solver, JCG solver, or the Block Lanczos mode-extraction method are available.
- Power Dynamics: This method is used for very large models having DOFs more than 100000 and especially useful to find the first several modes.
- Reduced (Householder) method: Since this method uses reduced system matrices to calculate the solution, it is faster than the subspace method.
- Unsymmetric: The unsymmetric method is used for problems with unsymmetric matrices.

In this study, subspace method is selected to find the natural frequencies of the finite element model.

Finite element model of the shell is modeled by SHELL99 due to the first-order shear deformation theory. This finite element has eight nodes as shown in Figure 2.10.

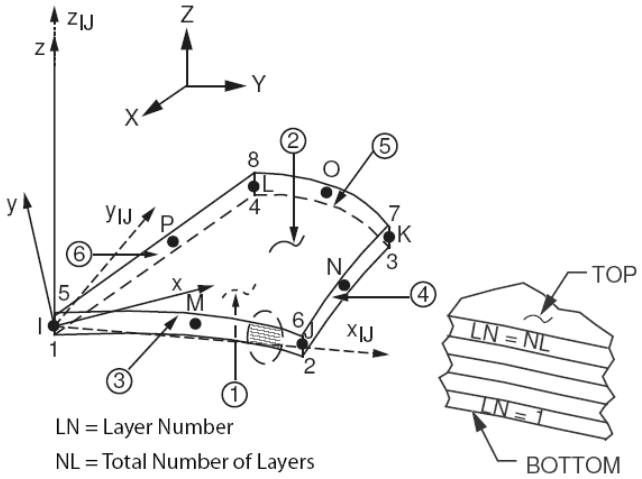

Figure 2.10. SHELL99 finite element
(Source: ANSYS Inc, 2007)

At each node, SHELL99 has six freedoms {UX, UY, UZ, ROTX, ROTY, ROTZ}. Moreover, SHELL99 is used for layered applications as illustrated in Figure 2.10. The element is defined by average or corner layer thicknesses, layer material direction angles, and orthotropic material properties. However, SHELL99 has assumptions and restrictions. Some of these are given below:

- Shear deflections are included in the element, however, normals to the center plane before deformation are assumed to remain straight after deformation.
- The stress varies linearly through the thickness of each layer.
- Interlaminar transverse shear stresses are based on the assumption that no shear is carried at the top and bottom surfaces of an element.

Finite element model of the stiffener in this study is modeled by BEAM188. This finite element is defined by nodes I, J, and K in the global coordinate system in Figure 2.11. Node K is used to define the orientation of the element.

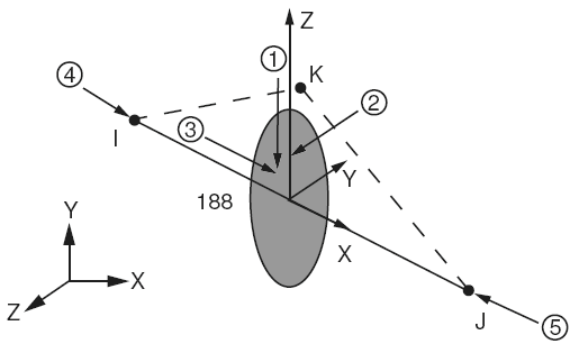

Figure 2.11. BEAM188 finite element
(Source: ANSYS Inc, 2007)

BEAM188 has six freedoms {UX, UY, UZ, ROTX, ROTY, ROTZ} at each node, Therefore, it is appropriate to use as stiffener with SHELL99.

BEAM188 is suitable for analyzing slender to moderately stubby/thick beam structures. This element is based on Timoshenko beam theory. Shear deformation effects are included.

Cross-section of the stiffener is defined by using the command SECTYPE along with BEAM188. Rectangular and I-shaped section are selected as beam cross section subtypes in this command.

CHAPTER 3

NUMERICAL RESULTS AND DISCUSSIONS

3.1. Case Studies for Verification of Finite Element Model

Several case studies are presented step by step in this section to verify the finite element model developed in ANSYS.

First case study is selected as vibration of composite square plate of which geometry is shown in Figure 3.1. Geometrical and material properties are given as

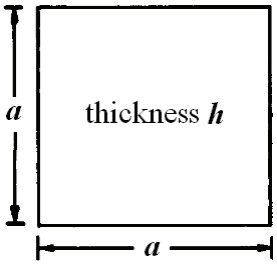

Figure 3.1. Square plate

$$\begin{aligned} &E_1 = 25E_2; \\ &G_{23} = 0.2E_2; \\ &G_{13} = G_{12} = 0.5E_2; \\ &\upsilon_{12} = 0.25 \end{aligned} \tag{3.1}$$

$$K_1^2 = K_2^2 = 5/6 \tag{3.2}$$

$$a/h = 100 \tag{3.3}$$

Linear layered structural shell element SHELL99 in ANSYS is selected for finite element modelling of shell. The numbers of elements in both directions used to model the structure are determined after trying several numbers of elements to mesh it by looking to desired value of non-dimensional fundamental frequencies given by Reddy (1984). Thus, 10x10 SHELL99 are used to model the square plate.

The present non-dimensional fundamental frequencies $\overline{\omega} = \omega\, a^2 \sqrt{\rho / E_2}\,/\,h$ obtained from ANSYS and the results from Reddy (1984) are given in Table 3.1 for comparisons. Thus, the present model is confirmed for this case.

Table 3.1. Comparison of the present non-dimensional fundamental frequencies with ones in the literature

Layers	0º/90º/0º	0º/90º/90º/0º
Reddy (1984)	15.183	15.184
Present	15.164	15.164

Second case study is selected as vibration of composite cylindrical shell shown in Figure 3.2 and having the same numerical data with the first case study except R_2.

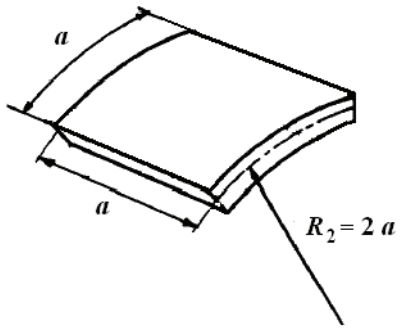

Figure 3.2. Cylindrical shell

The present non-dimensional fundamental frequencies $\overline{\omega} = \omega\, a^2 \sqrt{\rho / E_2}\,/\,h$ obtained from ANSYS by using again 10x10 SHELL99 mesh and the results from Reddy (1984) are given for comparisons in Table 3.2. Thus, the present model is confirmed for second case too.

Table 3.2. Comparison of the present non-dimensional fundamental frequencies with ones in the literature

Layers	0º/90º/0º	0º/90º/90º/0º
Reddy (1984)	36.770	36.858
Present	36.252	36.362

Third case study is selected as vibration of square plate shown in Figure 3.3.

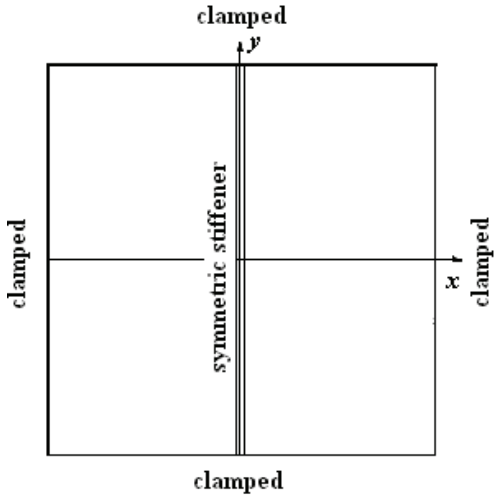

Figure 3.3. Clamped square plate with stiffener
(Source: Nair and Rao, 1984)

Geometrical and material properties of stiffened plate shown in Figure 3.3 are given by Nair and Rao (1984) and Palani et al (1993) below:

- dimensions of plate : 600x600x1 mm,
- dimensions of stiffener : 3.31x20.25x600 mm,
- Young modulus of plate and stiffener : E=6.87x104 MPa,
- Density of of plate and stiffener : ρ=2.78x10-6 kg/mm3,
- Posison ratio of plate and stiffener : ν=0.34

In order to provide the continuity condition between shell and stiffeners, BEAM44, which has also six degrees of freedom at each node, is used to model the stiffeners. It is a uniaxial element with tension, compression, torsion, and bending capabilities. Two mesh types as 10x10 and 20x20 are used to find the natural frequencies as Hz in this case study.

Table 3.3 and 3.4 show the comparison of present results with the results of STIFPT1 developed by Nair and Rao (1984). STIFPT1 uses a triangular plate bending element for the panel with the nodal freedoms $\{w, w_x, w_y, w_{xx}, w_{xy}, w_{yy}\}$ and beam element with the nodal freedoms $\{w, w_x, w_y, w_{xy}, w_{yy}\}$. However, SHELL99 has nodal freedoms {UX, UY, UZ, ROTX, ROTY, ROTZ}.

Table 3.3. Comparison of natural frequencies of unstiffened plate

Mode No	*f* [Hz] by STIFPT1	Present *f* [Hz] 10x10	Present *f* [Hz] 20x20
1	24.27	24.292	24.272
2	49.51	49.616	49.501
2	49.51	49.616	49.501
3	73.04	73.555	72.992
4	88.77	89. 686	88.742
5	89.24	89.134	89.171
6	111.48	112.95	111.31
6	111.48	112.95	111.31
7	142.22	143.51	142.01
7	142.21	143.51	142.01
8	149.00	152.98	148.49

Table 3.4. Comparison of natural frequencies of stiffened plate

Mode No	*f* [Hz] by STIFPT1	Present *f* [Hz] 10x10	Present *f* [Hz] 20x20
1	50.45	55.586	55.421
2	63.71	63.877	63.649
3	75.16	82.223	81.337
4	85.50	86.661	85.395
5	113.69	121.41	118.65
6	120.89	124.46	120.63

It can be said from the comparisons of the results in Table 3.3 and 3.4 that results of the present model are in good agreement with the results in literature.

Finally, fourth case study is selected as vibration of paraboloidal shell studied by Tornabene and Viola (2008). The geometry of the shell of revolution with a parabolic curved meridian shown in Figure 3.4 can be expressed analytically as follows:

$$R_0^2 - [(s_1^2 - d^2)/S]x_3 = 0 \tag{3.4}$$

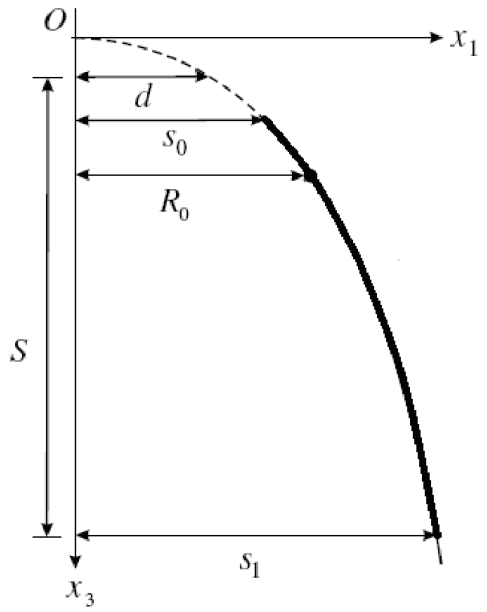

Figure 3.4. Geometry of paraboloidal shell of revolotion

Numerical values of the geometry of paraboloidal shell of revolotion based on Figure 3.4 are detailed as: d=0, S=2 m, s_0=1 m, s_1=4 m and thickness h=0.1 m.

Material properties of the paraboloidal shell are given by Tornabene and Viola (2008) as

- Young modulus of shell : E=2.1x1011 Pa,
- Density of of shell : ρ=2.1x1011 kg/m3,
- Poisson's ratio of shell : ν=0.3
- Shear factor : χ=6/5.

The paraboloidal shell of revolution shown in Figure 3.5 is geometrically modeled in APDL code ANSYS by using Equation (3.4). As seen from Figure 3.5 that upper and lower circles have four segments. Also, its upper edge is fixed.

In order to decide the minimum number of element in axial and circumferential directions of the paraboloidal shell of revolution, convergence of first natural frequencies of it is studied by using different meshes. The selected mesh having N=7 and 4 times N elements in axial and circumferential directions, respectively, is shown in Figure 3.6 by considering the convergence curve of first natural frequencies shown in Figure 3.7.

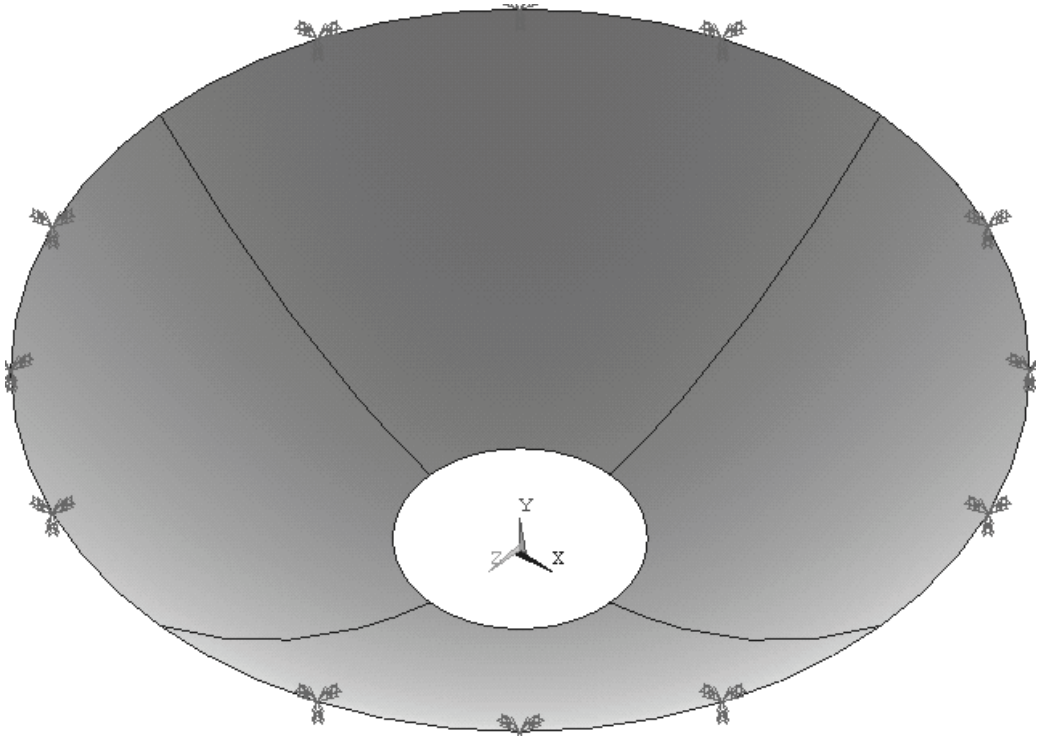

Figure 3.5. Geometrical model of paraboloidal shell

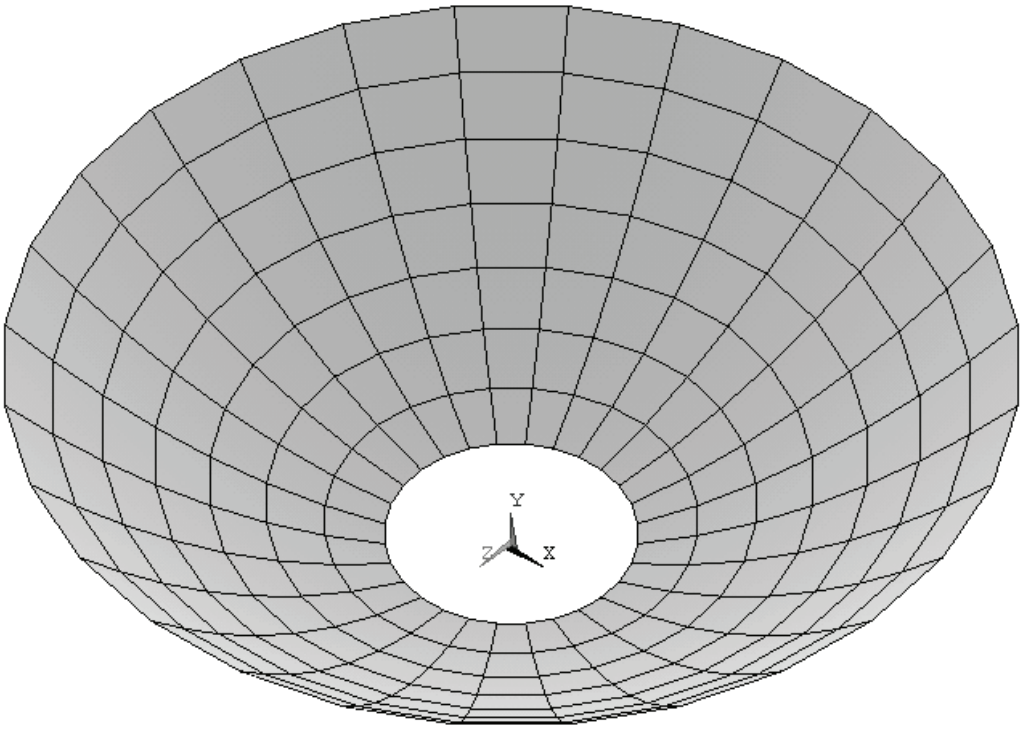

Figure 3.6. Finite element model of paraboloidal shell with SHELL99

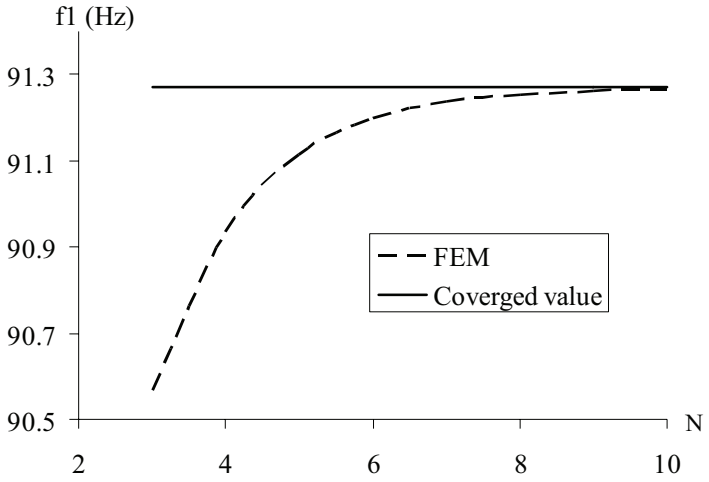

Figure 3.7. Convergence curve of first natural frequencies of paraboloidal shell

Present natural frequencies and the results of Tornabene and Viola (2008) are given in Table 3.5 including the number of elements and element types. GDQ in Table 3.5 are initials of the Generalized Differential Quadrature. It should be mentioned that Shell93 is not used for layered applications.

Table 3.5. Comparison of natural frequencies of paraboloidal shell of revolution

Mode No	Present f [Hz] 7x28 Shell99	f [Hz] given by Tornabene and Viola (2008)		
		GDQ Method 21x21	ABAQUS 28x28 S8R6	ANSYS 28x28 Shell93
1	91.24	91.24	91.29	91.28
2	91.24	91.24	91.29	91.28
3	131.50	131.29	131.39	131.49
4	131.50	131.29	131.39	131.49
5	155.40	154.90	155.12	155.29
6	155.40	154.90	155.12	155.29
7	158.02	157.99	158.12	158.02
8	158.02	157.99	158.12	158.03
9	170.48	169.66	169.84	170.21
10	170.48	169.68	169.84	170.21

It is seen from Table 3.5 that the first and second natural frequencies of the present model are in very good agreement with the results given for GDQ Method.

The definition of percentage difference given below can be used to discuss the other comparisons.

$$\%\ \text{difference} = \frac{|v_1 - v_2|}{(v_1 + v_2)/2} 100 \tag{3.5}$$

Maximum percentage difference for first natural frequencies is 0.0548.

3.2. Paraboloidal Shell with Stiffeners

The geometrical model of paraboloidal shell used in fourth case study is selected to add stiffeners. Laminated composite with laminate code 0º/90º/90º/0º is selected for that paraboloidal shell. Material properties of shell is obtained by taking E_2=7000 MPa in Equation (3.1). Also density of shell is considered as ρ_{shell}=7.85x10^{-9} ton/mm^3. Rectangular and I cross-sections are used for stiffeners in order to see the effects of cross-section of stiffereners on natural frequencies. Aluminum is selected for material of the stiffereners. Material properties of aluminum given in the third case study are used for stiffeners.

The paraboloidal shell and stifferners are meshed by SHELL99 and BEAM188, respectively. Finite element models of a paraboloidal shell with four and eigth rectangular cross-sectioned stiffereners are shown in Figures 3.8 and 3.9. Also, finite element models of a paraboloidal shell with four and eigth I cross-sectioned stiffeners are shown in Figures 3.10 and 3.11. Rectangular cross-sectioned sfiffener has 40x200 mm dimensions for width x height. Geometrical data for cross-section of I-type stiffener is given in Figure 3.12.

In order to mesh the meshed paraboloidal shell with four stiffeners, node numbers of the paraboloidal shell in the planes *xy* and *yz* shown in Figure 3.8 are used. It can be seen from Figure 3.8 that the axial edges of SHELL99 are located in these planes. Therefore, each axial edge of SHELL99 in these planes has two BEAM188 elements. However, to mesh the meshed paraboloidal shell with eight stiffeners, node numbers of the paraboloidal shell in the eight planes equally distributed about the axis *y* are used as seen in Figure 3.9. In this case, fifth to eighth stiffeners are located in the nodes of the SHELL99 having nodes on edges in circumferential directions. Thus, each SHELL99 element in these directions has only one BEAM188 as shown in Figure 3.9.

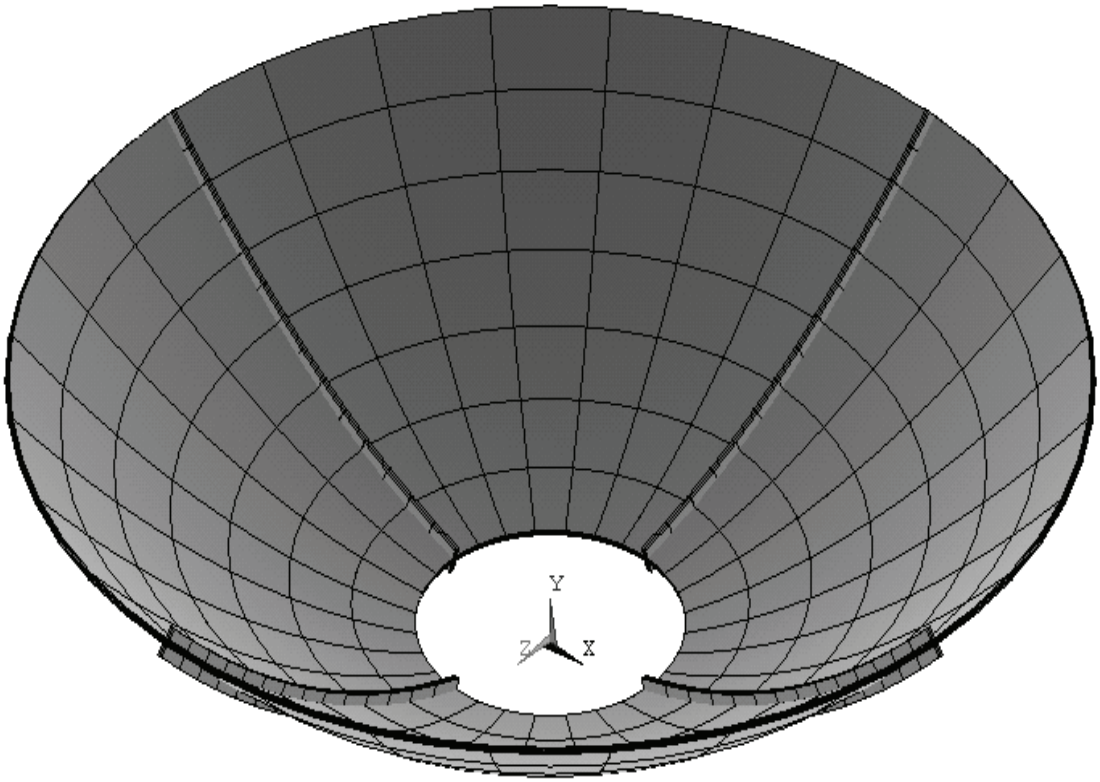

Figure 3.8. FEM of a paraboloidal shell with 4 rectangular cross-sectioned stiffereners

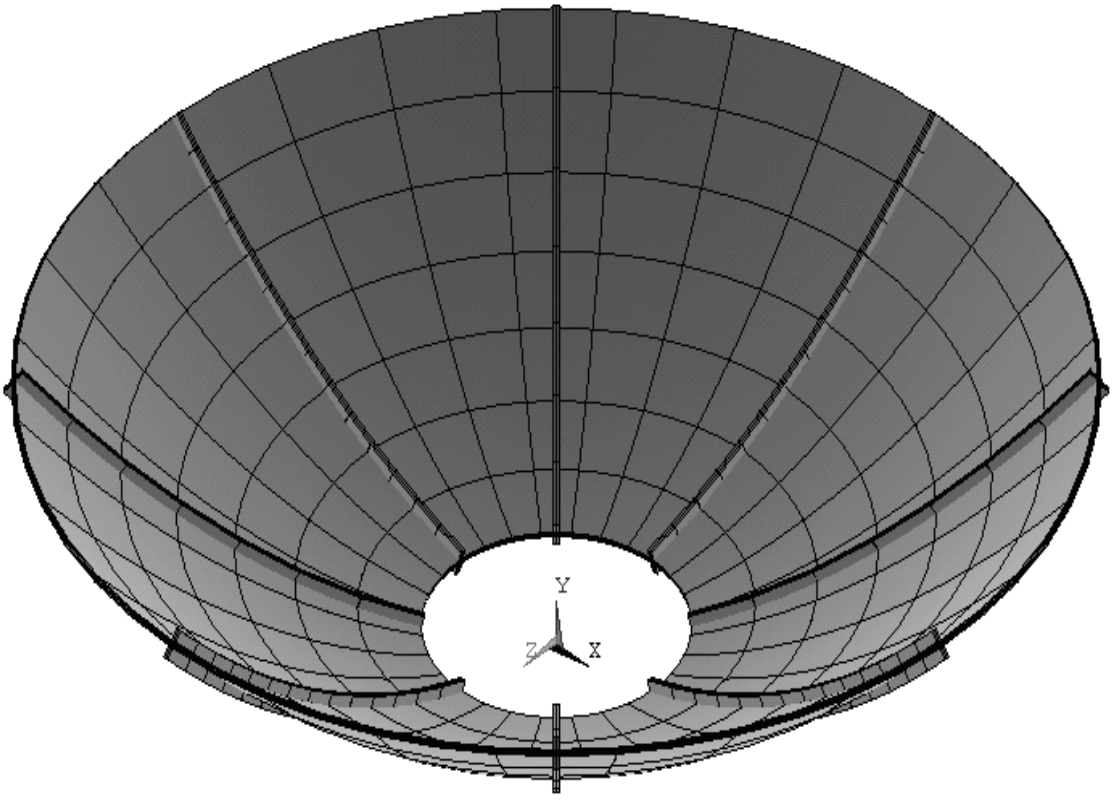

Figure 3.9. FEM of a paraboloidal shell with 8 rectangular cross-sectioned stiffereners

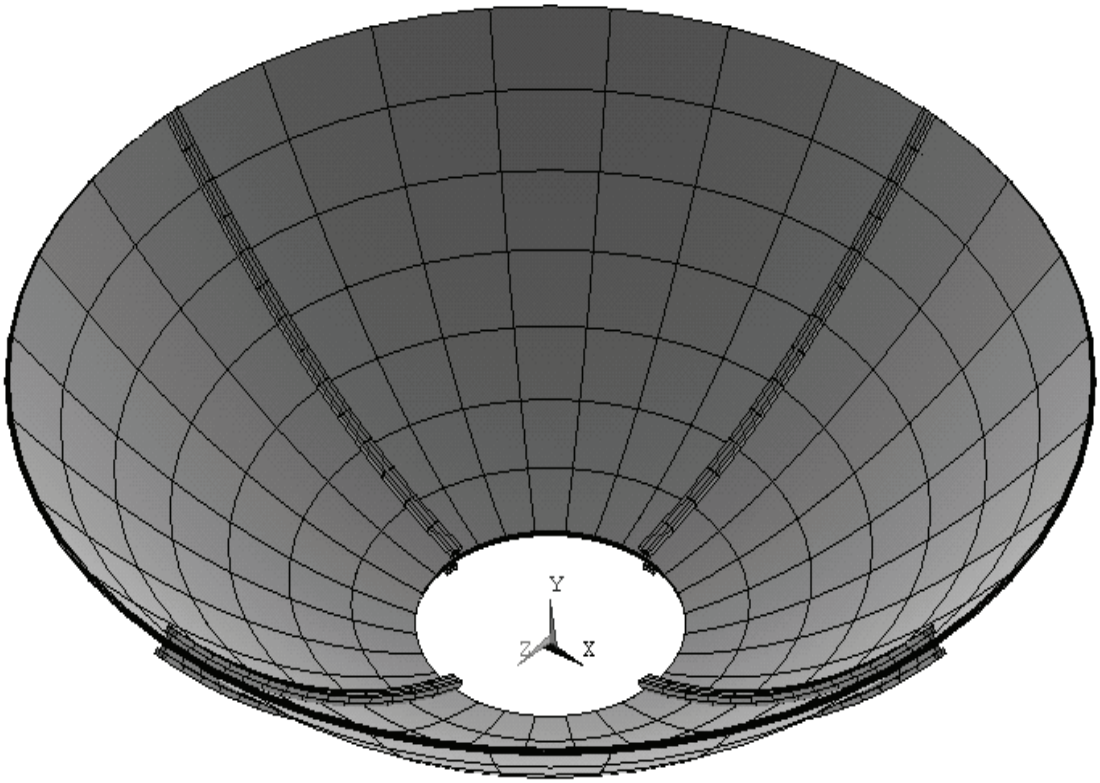

Figure 3.10. FEM of a paraboloidal shell with 4 I cross-sectioned stiffereners

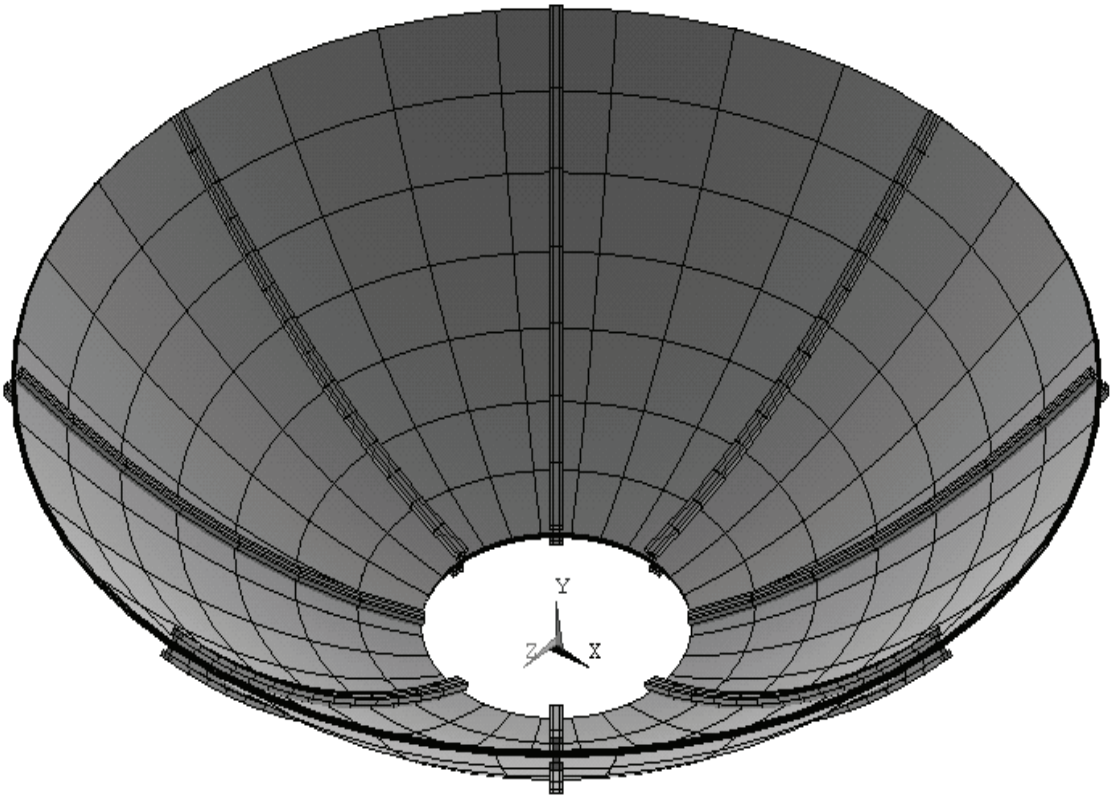

Figure 3.11. FEM of a paraboloidal shell with 8 I cross-sectioned stiffereners

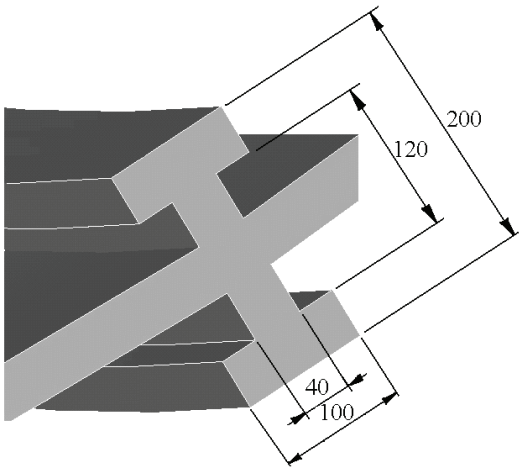

Figure 3.12. Cross-sectional data for I type stifferener

Natural frequencies of paraboloidal shell with different types of stiffeners are given in Table 3.6.

Table 3.6. Natural frequencies *f* [Hz] of paraboloidal shell with different stiffeners

Mode No	Shell without stiffeners	Shell with 4 rectangular stiffeners	Shell with 8 rectangular stiffeners	Shell with 4 I stiffeners	Shell with 8 I stiffeners
1	19.374	19.338	19.660	19.356	19.835
2	19.422	19.776	19.719	19.971	19.907
3	26.520	26.917	27.226	27.123	27.544
4	26.520	26.917	27.226	27.123	27.544
5	42.211	42.009	41.695	41.931	41.060
6	42.111	42.009	41.815	41.931	41.664
7	43.106	42.386	41.815	42.045	41.664
8	43.119	44.037	44.826	44.529	45.625
9	46.374	47.256	48.042	47.844	49.002
10	46.374	47.256	48.042	47.844	49.002

The following discussions can be drawn from Table 3.6:

- Shell with stiffener has higher natural frequencies than without ones except modes 1, 5, 6, and 7.
- The number of stiffener and the stiffener type has not common effect on natural frequencies.

- Due to the double mass in the stiffener axis based on SHELL99 and BEAM188, it is not possible to compare the unstiffened and stiffened ones.
- Moreover, it is not possible to compare the effects of number of stiffener on natural frequencies due to the reason given above.
- I-type stiffener has more effect than rectangular cross-sectioned stiffener on first to fourth and eighth to tenth natural frequencies of both four and eight stiffened paraboloidal shell.
- Since the paraboloidal shell is obtained from the revolution of the parabola defined by the Equation (3.4), natural frequencies of even and odd numbered modes are almost equal to each other.

Mode shapes of stiffened paraboloidal shell shown in Figure 3.8 are illustrated in Figures 3.13-3.22.

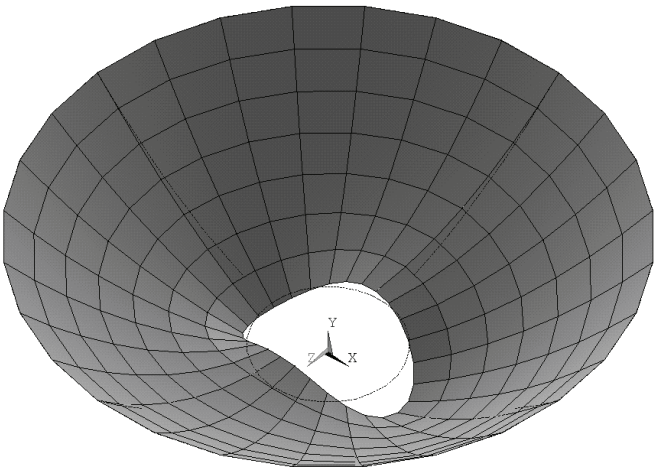

Figure 3.13. First mode shape of stiffened paraboloidal shell shown in Figure 3.8

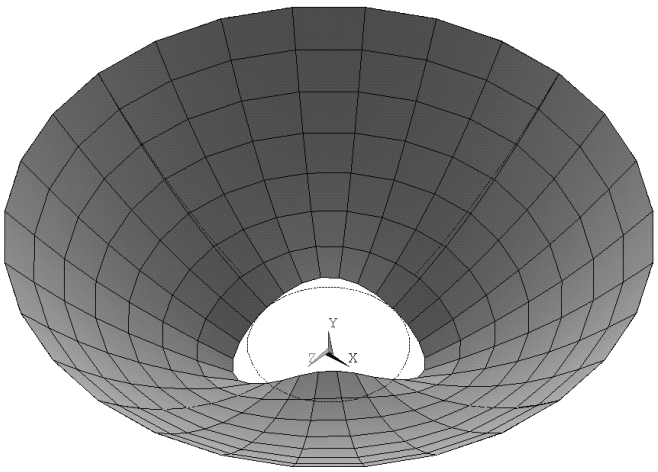

Figure 3.14. Second mode shape of stiffened paraboloidal shell shown in Figure 3.8

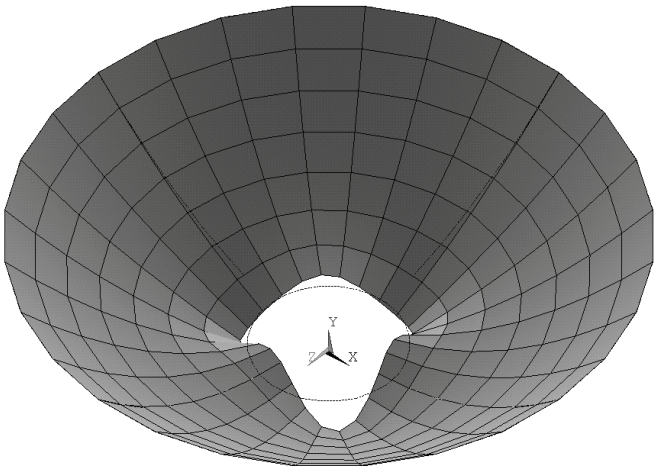

Figure 3.15. Third mode shape of stiffened paraboloidal shell shown in Figure 3.8

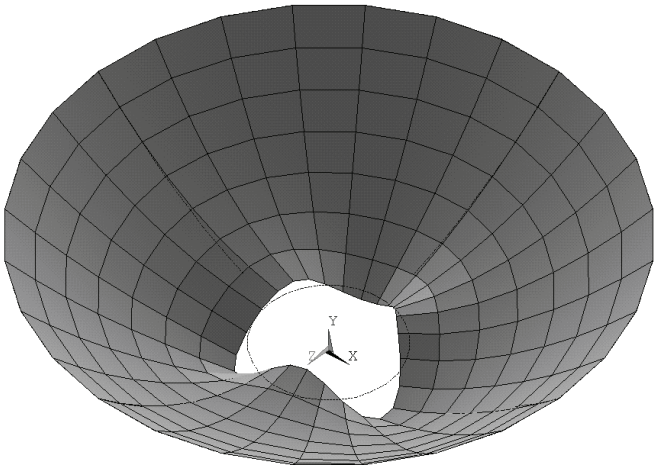

Figure 3.16. Fourth mode shape of stiffened paraboloidal shell shown in Figure 3.8

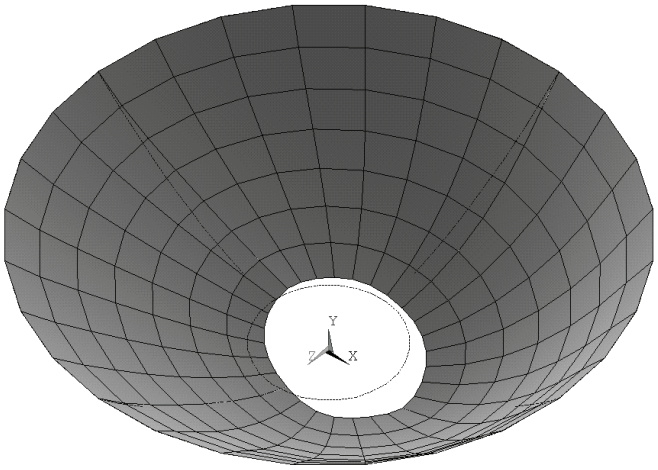

Figure 3.17. Fifth mode shape of stiffened paraboloidal shell shown in Figure 3.8

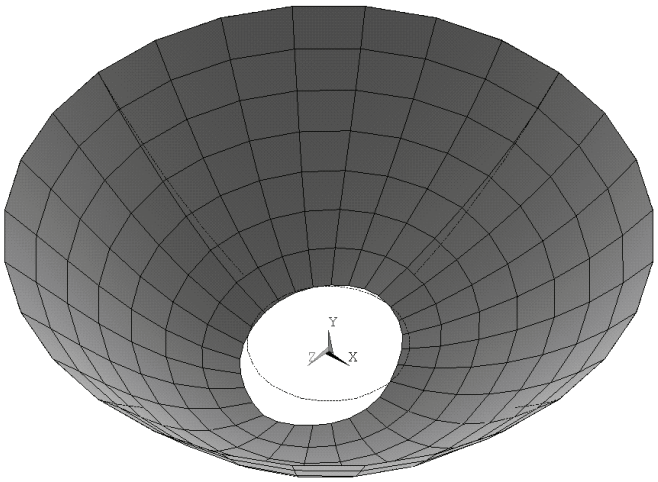

Figure 3.18. Sixth mode shape of stiffened paraboloidal shell shown in Figure 3.8

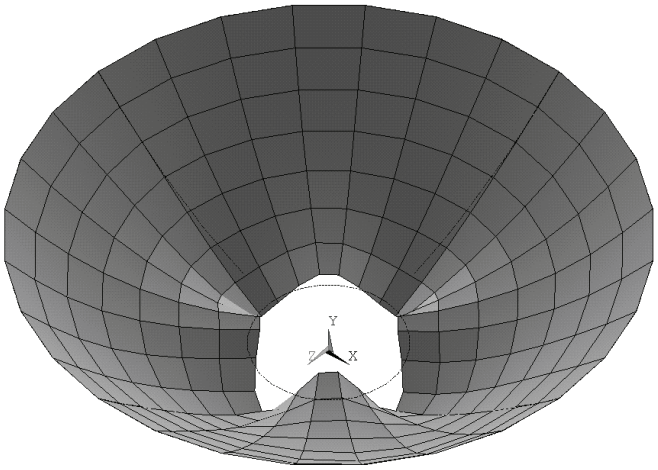

Figure 3.19. Seventh mode shape of stiffened paraboloidal shell shown in Figure 3.8

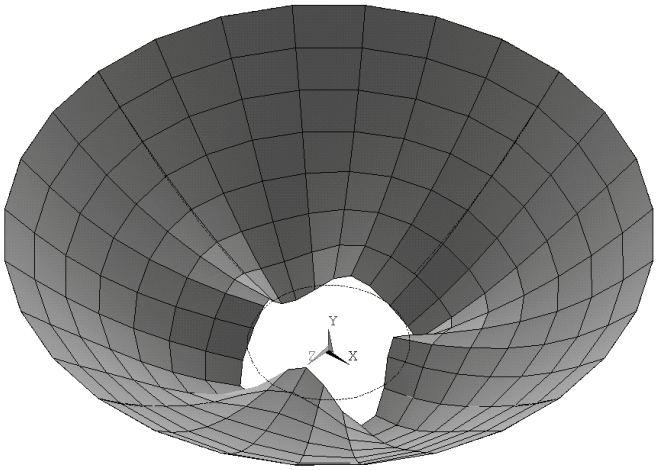

Figure 3.20. Eighth mode shape of stiffened paraboloidal shell shown in Figure 3.8

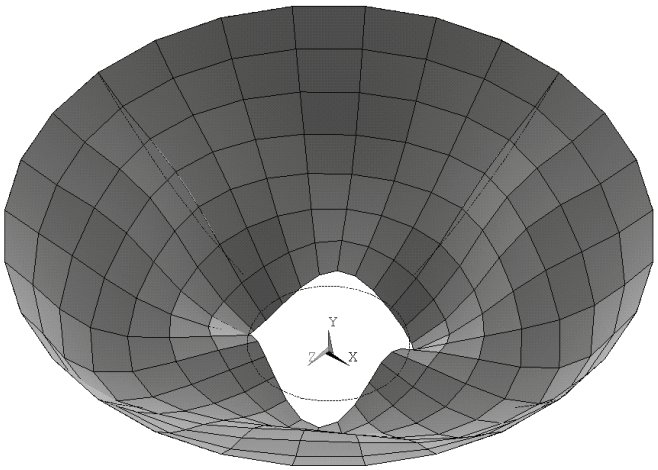

Figure 3.21. Nineth mode shape of stiffened paraboloidal shell shown in Figure 3.8

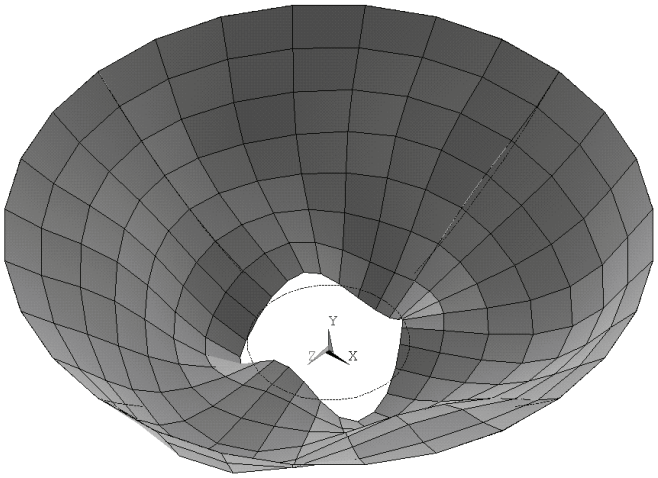

Figure 3.22. Tenth mode shape of stiffened paraboloidal shell shown in Figure 3.8

CHAPTER 4

CONCLUSIONS

Vibration characteristics of fiber-reinforced and laminated composite paraboloidal shells with stiffeners are studied with a computer code developed by using APDL (ANSYS Parametric Design Language) in ANSYS which is a finite element software. The developed code is verified by using several results available in the reachable literature.

The effects of stiffeners on natural frequencies are investigated by selecting different number of stiffener in different geometries. It is found that I-type stiffener is more effective than the rectangular cross-sectioned stiffener for first to fourth and eighth to tenth natural frequencies of both four and eight stiffened paraboloidal shell. Thus, it can be said that the number of stiffener and the stiffener type has not common effect on natural frequencies.

REFERENCES

ANSYS Inc, 2007. ANSYS Elements reference Release 11.0, Canonsburg PA.

Bacon, M.D. and Bert C.W. 1967, Unsymmetric free vibrations of orthotropic sandwich shells of revolution, *AIAA Journal* 5: 413-417.

Bert, C.W. and Kim, C.D. 1993, Vibration of composite-material cylindrical shells with ring and/or stringer stiffeners, *Composite Structures* 25: 477-484.

Bhimaraddi, A., Carr, A.J. and Moss P.J. 1989, Finite element analysis of laminated shells of revolution with laminated stiffeners, Computers & Structures 33: 295-305.

Cook, R.D, Malkus, D.S., and Plesha, M.E. 1989, Concepts and applications of finite element analysis. New York: John Wiley and Sons, Inc.

Edalat, P., Khedmati, M.R. and Soares, C.G. 2013, Free vibration and dynamic response analysis of stiffened parabolic shells using equivalent orthotropic shell parameters, *Latin American Journal of Solids and Structures* 10: 747-766.

Egle, D.M. and Sewall, J.L. 1968, An analysis of free vibration of orthogonally stiffened cylindrical shells with stiffeners treated as discrete elements, *AIAA Journal* 6: 518-526.

Flügge, W. 1934, Stress in shells, Springer, Berlin.

Flügge, W. 1973, Stress in shells, Springer, Berlin.

Hartog, J.P.D., 1952, Advanced Strength of Materials, New York, McGraw-Hill.

Gan, L., Li, X. and Zhang, Z. 2009, Free vibration analysis of ring-stiffened cylindrical shells using wave propagation approach, *Journal of Sound and Vibration* 326: 633-646.

Goswami S. and Mukhopadhyay, M. 1994, Finite element analysis of laminated composite stiffened shell, *Journal of Reinforced Plastics and Composites* 13: 574-616.

Gunay, E. 1999, Finite element analysis of laminated stiffened cylindrical shallow shell, *Applied Composite Materials* 6: 381-395.

Hoppmann II, W.H., Cohen, M.I. and Kunukkasseril, V.X. 1963, Elastic vibrations of paraboloidal shells of revolution, *The Journal of the Acoustical Society of America* 36: 349-353.

Huang, S.C. and Chen, L.H. 1996, Vibration of a spinning cylindrical shell with internal/external ring stiffeners, *Journal of Vibration and Acoustics* 118: 227-236.

Jafari, A.A. and Bagheri, M. 2006, Free vibration of non-uniformly ring stiffened cylindrical shells using analytical, experimental and numerical methods, *Thin-Walled Structures* 44: 82-90.

Kaw, A.K. 2006. Mechanics of composite materials, Boca Raton, CRC Press.

QHA, 2017, http://qha.com.ua/tr/toplum/ukraynali-pilot-ucagini-kahramanca-turkiye-deki-piste-indirdi/157935/

Lee, Y.S. and Kim, Y.W. 1998, Vibration analysis of rotating composite cylindrical shells with orthogonal stiffeners, *Computers and Structures* 69: 271-281.

Liao, C.L. and Reddy, J.N. 1990, Analysis of anisotropic, stiffened composite laminates using a continuum-based shell element, *Computers and Structures* 34: 805-815.

Love A.E.H. 1934, Mathematical theory of elasticity, Cambridge University Press, 514.

Luan, Y., Ohlrich, M. and Jacobsen, F. 2011, Smearing technique for vibration analysis of simply supported cross-stiffened and doubly curved thin rectangular shells, *The Journal of the Acoustical Society of America* 129: 707-716.

Mikulas, M.M. and McElman, J.A. 1965, On free vibrations of eccentrically stiffened cylindrical shells and flat plates, NASA TN D-3010.

Mustafa, B.A.J. and Ali, R. 1989, An energy method for free vibration analysis of stiffened circular cylindrical shells, *Computers and Structures* 32: 355-363.

Nair, P.S. and Rao, M.S. 1984, On vibration of plates with varyinh stiffener length, *Journal of Sound and Vibration* 95: 19-29.

Naumann, E.C., Catherines, D.S. and Walton, W.C. 1971, Analytical and experimental studies of natural vibration modes of ring-stiffened truncated-cone shells with variable theoretical ring fixity, NASA TN D-6473.

Pan, Z., Li, X. and Ma, J. 2008, A study on free vibration of a ring-stiffened thin circular cylindrical shell with arbitrary boundary conditions, *Journal of Sound and Vibration* 314: 330-342.

Prokopenko, N.Ya. 1979, Intrinsic oscillations of a reinforced laminar cylindrical shell, *Soviet Applied Mechanics* 15: 42-49.

Prusty, B.G. and Satsangi, S.K. 2001, Analysis of stiffened shell for ships and ocean structures by finite element method, *Ocean Engineering* 28: 621-638.

Prusty, B.G. 2003, Linear static analysis of composite hat-stiffened laminated shells using finite elements, *Finite Elements in Analysis and Design* 39: 1125-1138.

Raj, D.M., Narayanan, R., Khadakkar, A.G., Paramasivam, V. 1995, Effect of ring stiffeners on vibration of cylindrical and conical shell models, *Journal of Sound and Vibration* 179: 413-426.

Reddy, J.N. 1984, Exact solutions of moderately thick laminated shells, *Journal of Engineering Mechanics* 110: 794-809.

Ruotolo, R. 2001, A comparison of some thin shell theories used for the dynamic analysis of stiffened cylinders, *Journal of Sound and Vibration* 243: 847-860.

Sewall, J.L. and Naumann, E.C. 1968, An experimental and analytical vibration study of thin cylindrical shells with and without longitudinal stiffeners, NASA TN D-4705.

Sinha, G. and Mukhopadhyay, M. 1995, Static and dynamic analysis of stiffened shells, *The Indian National Science Academy* 61: 195-219.

Soedel, W. 1971, Similitude approximations for vibrating thin shells, *The Journal of the Acoustical Society of America* 49: 1535-1541.

Srinivasan, R.S. and Krishnan, P.A. 1989, Dynamic analysis of stiffened conical shell panels, *Computers and Structures* 33: 831-837.

Tornabene, F., Viola, E., 2008. 2-D solution for free vibrations of parabolic shells using generalized differential quadrature method. *European Journal of Mechanics A/Solids* 27: 1001–1025.

Torkamani, S., Navazi, H.M., Jafari, A.A. and Bagheri, M. 2009, Structural similitude in free vibration of orthogonally stiffened cylindrical shells, *Thin-Walled Structures* 47: 1316-1330.

Venkatesh, A. and Rao, K.P. 1983, Analysis of laminated shells with laminated stiffeners using rectangular shell finite elements, *Computer Methods in Applied Mechanics and Engineering* 38: 255-272.

Venkatesh, A. and Rao, K.P. 1985, Analysis of laminated shells of revolution with laminated stiffeners using a doubly curved quadrilateral finite element, *Computers and Structures* 20: 669-682.

Yardimoglu, B. 2016. Lecture notes on Advanced Mechanics of Materials, Izmir: Izmir Institute of Technology.

Zhao, X., Liew, K.M. and Ng, T.Y. 2002, Vibrations of rotating cross-ply laminated circular cylindrical shells with stringer and ring stiffeners, *International Journal of Solids and Structures* 39: 529-545.